

NOAA Technical Report ERL 371-GLERL 12
(GLERL Contribution No. 77)



An Ecological Model for Lake Ontario Model Formulation, Calibration, and Preliminary Evaluation

Donald Scavia
Brian J. Eadie
Andrew Robertson

Great Lakes Environmental Research Laboratory
Ann Arbor, Michigan

June 1976

U. S. DEPARTMENT OF COMMERCE
Elliot Richardson, Secretary

National Oceanic and Atmospheric Administration
Robert M. White, Administrator

Environmental Research Laboratories
Wilmot Hess, Director



Boulder, Colorado

NOTICE

The NOAA Environmental Research Laboratories do not approve, recommend, or endorse any proprietary product or proprietary material mentioned in this publication. No reference shall be made to the NOAA Environmental Research Laboratories, or to this publication furnished by the NOAA Environmental Research Laboratories, in any advertising or sales promotion which would indicate or imply that the NOAA Environmental Research Laboratories approve, recommend, or endorse any proprietary product or proprietary material mentioned herein, or which has as its purpose an intent to cause directly or indirectly the advertised product to be used or purchased because of this NOAA Environmental Research Laboratories publication.

CONTENTS

	Page
ABSTRACT	1
1. INTRODUCTION	1
1.1 Objectives	2
1.2 Modeling Philosophy	3
1.3 Rationale for Space/Time Framework	3
2. DEVELOPMENT OF THE MODELING FRAMEWORK	3
2.1 Theoretical Framework for the Model	6
2.2 The Physical Model	8
2.3 Forcing Functions	9
2.4 Sedimentation	12
2.5 Biological System	14
2.5.1 Phytoplankton	17
2.5.2 Zooplankton	19
2.5.3 Detritus	19
2.5.4 Phosphorus	20
2.5.5 Nitrogen	20
2.5.6 Inorganic Carbon	21
2.5.7 Sediment/Benthic Fauna	23
3. PRELIMINARY EVALUATION	24
3.1 Process Simulation	27
3.2 State Variable Simulation	29
4. ANALYSIS OF MODEL OUTPUT	34
5. ANALYSIS OF MODEL FUNCTIONS	35
5.1 Diffusion	35
5.2 Sedimentation	36
5.3 Self-Shading	36
5.4 Fish Predation	37
5.5 Temperature	37
6. SUMMARY	39
7. REFERENCES	46
APPENDIX A. Model Coefficients and Initial Conditions	46
A.1 Phytoplankton Coefficients	47
A.2 Remineralization Constants	47
A.3 Zooplankton Coefficients	53
A.4 Initial Conditions	55
APPENDIX B. Model Equations	62
APPENDIX C. Computer Program	

FIGURES

	Page
1. The hydrodynamic system.	5
2. Predicted and observed average segment temperatures.	7
3. Predicted and observed segment thicknesses.	7
4. Modeled effect of growth limitation and shape correction on phytoplankton sinking rate.	12
5. Biological system.	13
6. Logic of benthic carbon calculations.	24
7. Predicted and observed primary production and epilimnion turnover rate.	25
8. Predicted community production: Respiration ratios for epilimnion and thermocline segments.	25
9. Predicted and observed epilimnion state variables.	28
10. Predicted and observed epilimnion state variables.	28
11. Predicted and observed hypolimnion state variables.	28
12. Predicted and observed pH.	28
13. Predicted and observed CO ₂ gas exchange.	29
14. Simulated epilimnetic state variable dynamics.	30
15. Simulated dynamics of the epilimnetic nitrogen system.	30
16. Simulated succession of epilimnion phytoplankton groups.	31
17. Simulated succession of epilimnion zooplankton groups.	32
18. Simulated PO ₄ concentration and seasonal dynamics of factors affecting PO ₄ .	32
19. Simulated NO ₃ concentration and seasonal dynamics of factors affecting NO ₃ .	33
20. Simulated large cladoceran concentration and seasonal dynamics of factors affecting large cladocerans.	33
21. Simulated small diatom concentration; nutrient, light, and temperature limitation; and seasonal dynamics of factors affecting small diatoms.	34
22. Accumulation and partitioning of sediment carbon and seasonal dynamics of the macrobenthos.	34

APPENDIX FIGURES

C.1. Model program logic flow.	63
--------------------------------	----

TABLES

Page

1. Predicted sinking rates.

26

APPENDIX TABLES

A.1. Phytoplankton coefficients.

47

A.2. Assimilation and preference coefficients.

48

A.3. Model coefficients.

51

B.1. Biological system.

55

AN ECOLOGICAL MODEL FOR LAKE ONTARIO MODEL FORMULATION, CALIBRATION, AND PRELIMINARY EVALUATION

Donald Scavia, Brian J. Eadie, and Andrew Robertson

A simulation model describing the dynamics of four types of phytoplankton, six types of zooplankton, detritus, organic nitrogen, ammonia, nitrate, available phosphorus, the carbonate system, and benthic invertebrates has been developed for the Lake Ontario ecosystem. The equations are described. The ecological model is driven by a physical model designed to predict average temperature, segment thicknesses, and vertical diffusion coefficients for the three-layer model.

In addition, an original formulation for calculating sedimentation rates is shown to accurately predict community settling rates. The simulated processes and predicted variables follow ecologically realistic patterns and compare favorably to measured parameters in Lake Ontario.

Sensitivity analyses revealed that modeled phosphorus was quite responsive to changes in diffusion, sedimentation was critical to predicting benthic dynamics, and self-shading by phytoplankton was not critical due to the relationship between light limitation and phosphorus depletion. Changes in temperature resulted in predicted shifts in the peaks of the phytoplankton and zooplankton, and the sensitivity of the model to fish predation indicated the need for better descriptions of fish dynamics.

1. INTRODUCTION

1.1 Objectives

The field phase of the International Field Year for the Great Lakes (IFYGL), a large multidisciplinary, interagency, international project, was carried out in 1972-73 (Ludwigson, 1974). One task included under IFYGL had as its goal the development of a generalized mathematical model of the Lake Ontario ecosystem. The report presented here documents this model and presents a preliminary evaluation of the results obtained with it.

This model was developed with two rather distinct objectives in mind. The first was to gain insight into the functional relations in the Lake Ontario ecosystem and to identify the areas of most serious deficiency in our knowledge. This identification is to be used to establish research needs and to set research priorities.

The second objective was to initiate the development of models to aid resource managers. This objective is long-range. Because ecological modeling has already shown great promise for application in solving resource

management problems (e.g., see Russell, 1975), it is hoped that the model reported here will be the first step in the development of a series of ecological models to provide managers with predictions of the environmental consequences of various alternative courses of action or inaction.

This report documents the model status at the completion of the first stage of development and reflects progress through November 1975. Further documentation and updates will be the subjects of additional publications.

1.2 Modeling Philosophy

The mathematical framework for this type of model is derived from empirical and theoretical relationships developed both in the field and in the laboratory. Since there exist few unifying hypotheses in ecology, ecological models tend to be site-specific and thus difficult to generalize to other bodies of water without extensive alterations. Difficulty is also encountered in obtaining the required rate parameters, forcing functions, and initial conditions for a single system. These often must be subjectively extrapolated from controlled laboratory experiments or field measurements at some "similar" location.

In spite of these difficulties, over the past 30 years several generalized functional relationships have emerged, including descriptions of the dynamics of phytoplankton communities based on environmental parameters such as light, temperature, nutrient availability, and grazing by higher trophic levels and of general zooplankton kinetics as functions of temperature, food density, and predation. While these relationships are subject to continual refinement, they appear to be soundly based and general enough to cover many situations.

With these functional relationships simulating the general trends of the lower parts of the food web, one can examine interrelationships for which information is unavailable or difficult to determine experimentally. Establishing their importance within the modeling framework can aid in the design of laboratory and field programs. This type of modeling then represents a qualitative and semi-quantitative approach to the understanding of ecological systems.

The need for large-scale aquatic models has been manifested in workshops and symposia designed to establish the state-of-the-art in modeling (e.g., Russel, 1975; Middlebrooks, Falkenberg, and Maloney, 1973). The applicability of such models has also been demonstrated in a few cases (O'Connor et al., 1975; Chen and Orlob, 1975). Most applied models include some mechanisms based on chemical and ecological theory; however many empiricisms still exist and limit their applicability. Through the development of models based on sound ecological theory, one can begin to create flexible, yet accurate, descriptions of these aquatic systems.

1.3 Rationale for Space/Time Framework

The data on which most relationships in aquatic ecology are based are low frequency observations collected on the time scale of days to weeks and usually for only part of the year. Even these limited data are, at best, only available for a few years.

In order to investigate a system on a time scale of less than 1 day, one would require high frequency observations, as well as the use of more complex model functions to account for diurnal effects and short-term responses (e.g., luxury uptake of nutrients, vertical migration, and diurnal feeding habits), a course of action we have rejected as impractical at this time.

To observe multiyear trends in the Lake Ontario system, a model coupling the simulation of physical transport to the ecological model should be employed because it is difficult to translate regional loads to whole-lake inputs. When running a one-dimensional ecological model for many years, one should be cautious since the effects of the loads are not spatially uniform and a lake-wide average is probably not suitable. Most of the limnological and ecological data at our disposal for Lake Ontario were collected at a limited number of stations visited during a series of cruises. Without the use of collection sites that were sampled simultaneously, it is impossible to obtain a complete verification or calibration for a complex time-varying, three-dimensional model, unless one assumes that all of the reaction-time constants in the model are of the same magnitude as the time delay between stations.

Thus, we feel that we have obtained cost effectiveness for increasing ecological understanding through the development and analysis of a one-dimensional model of the annual cycle. However, the development of a three-dimensional model will become increasingly important as applications of the model are attempted.

Spatial and time variations in water quality were measured during IFYGL for Lake Ontario. Data of this sort are necessary for two- or three-dimensional modeling. Since this type of data is scarce, it would be impossible to develop, calibrate, and validate a model independently. Development of a one-dimensional model at this time is a preliminary necessity for expansion to three dimensions.

2. DEVELOPMENT OF THE MODELING FRAMEWORK

2.1 Theoretical Framework for the Model

The model is designed around the framework of mass conservation which, in our case, takes the mathematical form

$$V \frac{\partial C}{\partial t} = V \frac{\partial}{\partial Z} \left[K \frac{\partial C}{\partial Z} \right] + VSc, \quad (2.1.1)$$

assuming no advection or horizontal diffusion,

where

- C = component of interest
- Sc = change of component C within volume V
- K = diffusivity coefficient
- t = time
- Z = depth
- V = volume.

For our model, composed of three time-variable segments, each of homogeneous composition (fig. 1), the following is correct:

$$V \frac{\partial}{\partial t} \int_1^2 C dz = VK \frac{\partial C}{\partial Z} \Big|_1^2 + V \int_1^2 Sc dz. \quad (2.1.2)$$

The volume (V) is replaced below with Z_i , the thickness of segment i, times a unit area. This expression can include special transfers, such as air/water boundary gas exchange and sedimentation. Upon integration, equation 2.1.2 then becomes

$$\frac{\partial C_i}{\partial t} = \frac{1}{Z_i} (A + D + S) + Sc, \quad (2.1.3)$$

where

- A = air/water transfer (see Section 2.5.6)
- D = net diffusion
- S = net sedimentation
- = $S_{i-1} - S_i$ (see Section 2.4)
- Sc = internal change
- Z_i = thickness of segment i

$$D = \begin{cases} K_1 \left\{ \frac{C_2 - C_1}{\Delta Z_1} \right\} & \text{for surface segment} \\ K_1 \left\{ \frac{C_1 - C_2}{\Delta Z_1} \right\} + K_2 \left\{ \frac{C_3 - C_2}{\Delta Z_2} \right\} & \text{for thermocline segment} \\ K_2 \left\{ \frac{C_2 - C_3}{\Delta Z_2} \right\} & \text{for bottom segment} \end{cases}$$

$$\Delta Z_i = \frac{Z_{i+1} + Z_i}{2} \quad (\text{see Section 2.2})$$

K_i = average diffusivity coefficient for segment i
(see Section 2.2).

HYDRODYNAMIC SYSTEM

ATMOSPHERE

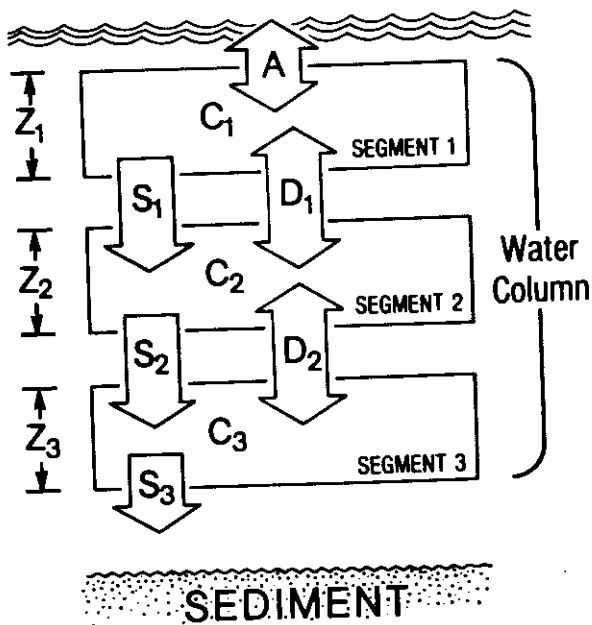


Figure 1. The hydrodynamic system: Z is segment thickness; S is sedimentation; D is diffusion; C is internal concentration; and A is air/water gas exchange.

Integration of equation 2.1.3 with respect to time results in

$$C_{i,n} - C_{i,n-1} = \frac{1}{Z_i} \int_1^2 (A + D + S) dt + \int_1^2 S_c dt \quad (2.1.4)$$

where

n = this time step
 $n-1$ = previous time step.

Numerically, the solution becomes

$$C_{i,n} = \left[C_{i,n-1} + \int_1^2 S_c dt \right] + \left[\frac{\Delta t}{Z_i} (D_{n-1} + A_n + S_n) \right] \quad (2.1.5)$$

where the left-hand bracket represents the new concentration due to biological and chemical changes within a segment and the remaining terms represent the physical transport into or out of the segments. (See Appendix C.)

2.2 The Physical Model

The calculation of thermal structure and vertical eddy diffusivity (K) is based on the work of Sundaram and Rehm (1973). In their model the equations governing the vertical turbulent transfer of heat are

$$\frac{\partial T}{\partial t} = \frac{\partial}{\partial Z} \left[K \frac{\partial T}{\partial Z} \right]$$

$$K = K_{He} (1 + \sigma_1 R)^{-1}$$

and

$$R = -a_v g Z^2 \frac{\partial T}{w_*^2},$$

where

- T = temperature
- t = time
- Z = the distance measured downward from the surface
- K = eddy diffusivity for the vertical transport of heat
- K_{He} = eddy diffusivity in the absence of stratification
- σ_1 = empirical constant
- a_v = volumetric coefficient of thermal expansion of water
- $\frac{g}{e}$ = acceleration due to gravity
- $w_* = \sqrt{r_s/e}$ = friction velocity due to the stress, r_s , exerted by the wind
- R = Richardson number.

The surface boundary condition could be calculated based on the thermal and mechanical energy crossing the air/water interface as is done by Sundaram and Rehm (1973); however, we have specified the annual cycle of surface water temperature (T) by the following equation derived from reported measurements (Pickett and Eadie, 1976):

$$T = 0.164 \times 10^{-9} t^5 - 0.128 \times 10^{-6} t^4 + 0.289 \times 10^{-4} t^3 - 0.13 \times 10^{-2} t^2 - 0.062 t + 4.328,$$

where t is the Julian date.

The initial water column temperature profile and the bottom boundary condition are assumed isothermal at 4°C. The physical model then can be used to calculate the temperature and diffusivity coefficients, K, for the remaining 11 vertical compartments. There are 12 compartments; the first 11 are each 4 m thick and the bottom 1 is 42 m thick. The level of the thermocline is set as the point of maximum temperature gradient, and three segments are created - an epilimnion and hypolimnion separated by the two 4-m compartments of the thermocline. During the unstratified portion of the year, the model defaults to three constant levels of 12, 20, and 54 m, respectively. The values for temperature and K are then the averages of the values for the individual 4-m segments within each level.

The calibrated physical model for Lake Ontario verifies well (fig. 2 and 3).

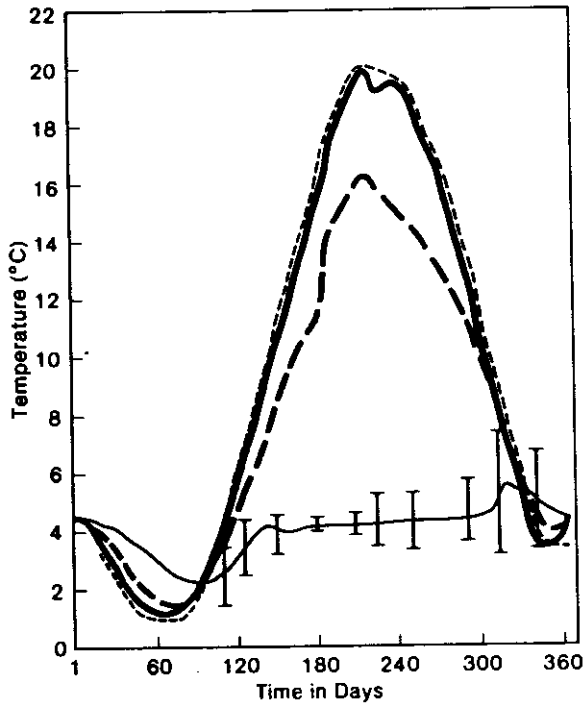


Figure 2. Predicted and observed average segment temperatures: Heavy solid line is epilimnion prediction and light dashed line is the 20-year climatological mean surface temperature; light solid line is hypolimnion prediction and bars represent lake-wide mean ± 1 standard deviation; heavy dashed line represents the predicted average thermocline temperature.

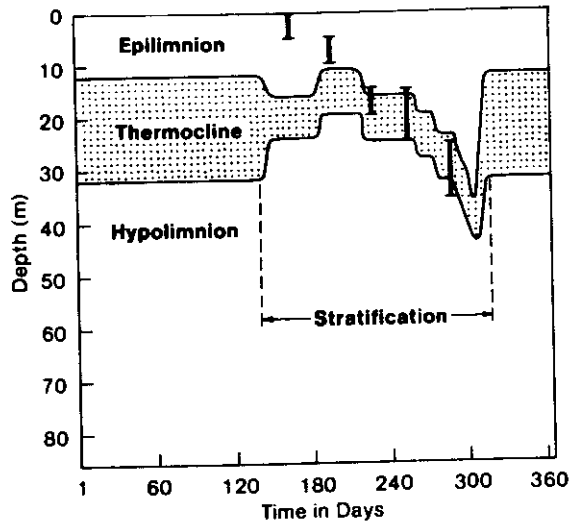


Figure 3. Predicted and observed segment thicknesses. Bars represent average thickness of thermocline during IFYGL (R. L. Pickett, personal communication).

2.3 Forcing Functions

The ecological model is driven by several forcing functions; two of these, temperature and turbulent diffusivity, are generated by the physical model (Section 2.2). A third, solar radiation, is based on linear interpolations of weekly averages obtained from a model developed by Atwater et al. (1973). A fourth, daily photoperiod, is calculated from a Fourier regression equation derived from monthly means obtained from weather summaries published during IFYGL [Department of Environment (Canada), Atmospheric Environment Service, 1972-73] and is as follows:

$$\begin{aligned}
 FP = & \{12.09 - 3.06*\text{Cos}(wt) + 0.8914*\text{Sin}(wt) \\
 & + 0.06604*\text{Cos}(w2t) - 0.0314*\text{Sin}(w2t) - 0.032*\text{Cos}(w3t) \\
 & + 0.052*\text{Sin}(w3t)\}/24, \qquad (2.3.1)
 \end{aligned}$$

where $w = 2\pi/365$
 $t = \text{time.}$

The gas exchange processes described later in Section 2.5.6 are controlled, in part, by surface wind. Wind velocities are approximated by

$$W_s = W_1 * F/3,$$

where W_s = wind at water surface
 W_1 = wind at 10 m over land
 $= 13.36 - 0.058t + 1.4*10^{-4}t^2$ (2.3.2)
 F = correction to 10 m over water
 $= 2.2 - 0.0082t + 2.29*10^{-5}t^2$ (2.3.3)
 t = Julian date.

A factor of one-third is used to estimate the overwater correction from 10-m winds to 10-cm winds and equations 2.3.2 and 2.3.3 are results of regressions of data from Department of Environment (Canada), Atmospheric Environment Service (1972-73) and Richards et al. (1966), respectively.

In this implementation of our model, external chemical and biological loads are not included. Two recent simulation studies on large lake ecosystems (Lake Ontario - Thomann et al., 1975; Lake George, N.Y. - Scavia and Park, 1976) suggest that allochthonous loads to open-water zones are relatively unimportant for determining seasonal dynamics. However, before employing this model as an engineering tool requiring multiyear simulations, these inputs must be included, as the yearly trends are important.

2.4 Sedimentation

A significant fraction of photoplankton population dynamics can be attributed to sinking (Lund, 1959). The importance of this process relative to nutrient uptake and primary production has been reviewed by Munk and Riley (1952) and Pasciak and Gavis (1974). This loss of epilimnetic material supplies carbon to both hypolimnetic animals (e.g., Mysis relicta) and benthic organisms. Models of phytoplankton dynamics and especially "whole ecosystem" models would certainly be incomplete without this process.

Attempts to model sinking have taken many forms. Some works approximate losses due to sinking by a constant average percent lost per day (Chen and Orlob, 1975; Thomann et al., 1975). Others have used linear functions of temperature (Scavia and Park, 1976) based on experimental rate measurements (Hutchinson, 1967; Smayda, 1974). One model attempts to mimic reduced sinking rates through the thermocline by utilizing a forcing function as follows:

$$S = \text{fn} \left[e^{k \frac{dT(t)}{dZ}} \right]$$

where $\frac{dT(t)}{dZ}$ is the time-dependent, maximum negative thermal gradient (Bloomfield et al., 1973).

Constant settling velocities result in overestimates at some times during the year and in underestimates at other times. Functions of temperature can approximate only one or two of the many contributing factors. Canale et al. (1975) avoid both constructs by using a known (or estimated) variation in sinking rate through time, but as they point out, these data are scarce at best. We feel that determining seasonal variability in the sinking rate is very important and, therefore, model it dynamically.

Particles sink when their specific gravity is greater than that of the surrounding medium. The density of phytoplankters, as well as that of water, varies during the year. Also, the density of the phytoplankton cells is species-specific. The model considers two types of phytoplankton and one detrital compartment. Live algal cells are considered to be 90 percent water and 10 percent organic matter. For green algae, we calculated the density of the organic fraction to be 1.27 g/cm³. Diatoms have relatively heavy siliceous frustules and therefore a greater density. The density of the siliceous shells is taken as 2.1 g/cm³. Large diatoms will have less silica relative to total volume than small diatoms if the cell wall is of constant thickness. Assuming a 1-μ frustule thickness, the organic fraction (by weight), calculated from shell geometry, is 43 percent silica for the small diatoms (based on the dimensions of Stephanodocus astrea v. minutula), and 7 percent for large diatoms (based on Melosira islandica subsp. helvetica). Detrital material is considered 100 percent organic matter (1.27 g/cm³).

The density (ρ) of phytoplankton is then calculated as

$$\rho = 0.9\rho_{H_2O} + 0.1\rho_{om},$$

where ρ_{H_2O} = density of water calculated from data in Weast (1973)
 $= 1.0 - 6.8 \times 10^{-6} * (T-4)^2 + 0.0011 \left(\frac{Z}{25000} \right)$
 T = temperature ($^{\circ}C$)
 Z = depth (cm)
 ρ_{om} = density of organic fraction, that is:
 $0.57(1.27) + 0.43(2.1)$ for small diatoms,
 $0.93(1.27) + 0.07(2.1)$ for large diatoms,
 1.27 for non-diatoms.

From this information, settling velocities can be calculated by Stokes Law

$$SV = \frac{2}{9} * g \frac{D^2}{\nu} * \left[\rho - \rho_{H_2O} \right],$$

where g = gravitational acceleration
 D = particle diameter (spherical)
 ν = viscosity of water calculated from data in Weast (1973)
 $= \rho_{H_2O} * (0.069T^2 - 5.3T + 177.6) * 0.0001$
 T = temperature ($^{\circ}C$)
 ρ = density of particle
 ρ_{H_2O} = density of water.

This formulation is valid for inert spheroids with the only variables being viscosity and particle and water density (both functions of temperature). For our needs, however, two important factors are missing in this formulation: corrections for the form of the particle and its physiological condition.

The effects of size, shape, colony formation, and physiology on phytoplankton sinking and population dynamics have been discussed by Munk and Riley (1952) and reviewed by Smayda (1970). Experimental evidence for the effect of these factors has been demonstrated for marine algae (Smayda and Boleyn, 1965, 1966a,b) and more recently for limnetic forms (Smayda, 1974).

To account for form resistance to sinking, we have employed correction formulae developed for specific particle shapes settling at low Reynolds numbers (McNown and Malaika, 1950). These equations have been developed for ellipsoids of various relative semi-axis lengths, so we can approximate most phytoplankton geometries. The settling velocity can be corrected as

$$V = V_s / K,$$

where V_s = the settling velocity for a sphere with a diameter equal to the nominal diameter of the particle (Stokes velocity)
 K = the correction factor.

McNown and Malaika also suggest the nominal diameter be calculated as

$$D = 2(abc)^{1/3},$$

where a, b, and c are the semi-axes lengths. However, we have used the diameter for a sphere of equivalent volume, in an attempt to correct for cases where the actual organism is not closely approximated by an ellipse, and obtained

$$D = 1.24 V_{eq}^{1/3},$$

where V_{eq} is the equivalent volume.

The correction factor, K , is calculated from

$$K = 16/3D(\alpha + \beta),$$

where α and β are complicated functions of the semi-axes lengths (McNown and Malaika, 1950).

Typical correction factors range from 1 for spherical particles to about 3 for very long-chained cylindrical particles. The correction factors for the four phytoplankton groups in the model are based on the dimensions of the dominant species (Munawar et al., 1974) as follows:

- Small diatoms - Stephanodiscus astrea - 1.58
- Large diatoms - Melosira islandica - 2.36
- Small non-diatoms - Rhodomonas minuta - 1.15
- Large non-diatoms - Peridinium aciculiferum - 1.05

The correction factor for detrital material was arbitrarily set at 1.1.

To simulate changes in specific density based on physiological health of the phytoplankton, the growth limitation terms described later in Section 2.5.1 are used. By assuming that cells are healthiest when neither light nor nutrients are limiting, the sinking rate can be made a function of physiological state as follows:

$$v = \frac{V_s}{K} \left\{ \frac{C}{XK+C} \right\},$$

where

- V = calculated settling velocity
- V_s = Stokes velocity based on nominal diameter
- K^s = form correction
- XK = overall limitation term (0→1) (see U in equation 2.5.4)
- C = constant.

The extremes of this function are maximum sinking for "dead" cells and minimum for actively growing cells (fig. 4).

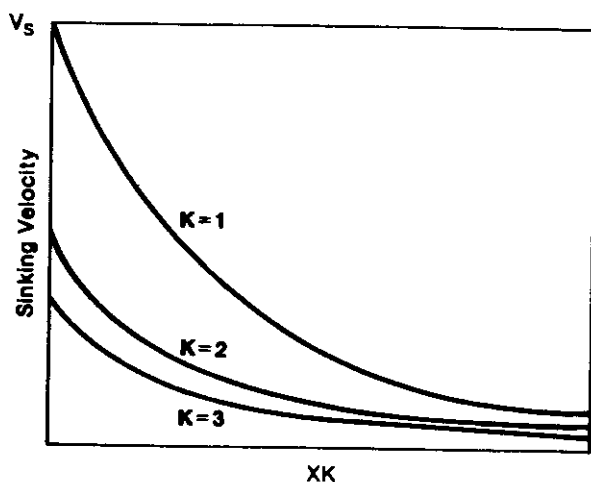


Figure 4. Modeled effect of growth limitation (XK) and shape correction (K) on phytoplankton sinking rate. V_s is Stokes velocity.

Evaluation of the construct relative to observed settling rates has not been completed; however, preliminary results are discussed below (Section 3.1).

2.5 Biological System

The biological portion of the model (fig. 5) is based on the movement of carbon through the food web; nitrogen and phosphorus are treated stoichiometrically.

In general, the system centers around the following four phytoplankton groups: large diatoms, small diatoms, large non-diatoms, and small non-diatoms. These groups are considered representative of the Lake Ontario assemblage; however, a blue-green algae compartment should be included when considering predictions concerning eutrophication. The phytoplankton take up carbon, phosphorus, and two forms of nitrogen (ammonia, preferentially) during primary production and release carbon through respiration. Phosphorus and organic nitrogen are released as respiratory by-products (excretion).

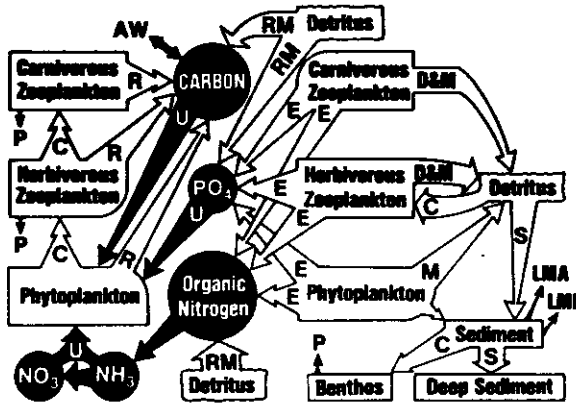


Figure 5. Biological system. C is consumption; R is respiration; U is nutrient uptake; RM is re-mineralization; P is fish predation; D is defecation; M is non-predatory mortality; E is excretion; S is sedimentation; AW is air/water gas exchange; and LMA and LMI are macrobenthic and microbenthic losses, respectively.

The phytoplankters are consumed by the following five categories of zooplankton: (1) small cladocerans, (2) large cladocerans, (3) herbivorous copepods, (4) mysids, and (5) rotifers. These strict herbivores are preyed upon by carnivorous zooplankton, and all six groups are eaten by a general consumer. This initial compartmentalization of zooplankton groups considers differences in feeding habits (cladocerans versus herbivorous copepods), as well as probable predatory pressures (large versus small cladocerans). The mysids are included to determine the effects of their dominance in the hypolimnion. When the carnivorous zooplankton group was included, it was found that their population could not be supported in the absence of the rotifers, quite possibly their most important food source.

A portion of the food taken in by each zooplankton group is assimilated and added to that group's carbon pool; the remainder is defecated and added to the detritus. The animals respire carbon and consequently release phosphorus and organic nitrogen. Detritus is either eaten by zooplankton or decomposed, resulting in inorganic carbon, phosphorus, and dissolved organic nitrogen, thus completing the nutrient cycles.

The phytoplankton groups and the detrital compartment also sink to the sediment, forming a sedimentary organic carbon compartment. Here, microbial activity removes a portion of the available carbon and the remainder is made available to the macrobenthos. Some sedimentary organic carbon is also lost to the deep, unavailable sediment.

The coefficient values and initial conditions of the model are in Appendix A. The equations describing the change of biotic and abiotic substances within each segment are given in Appendix B. The equations of the model are set up to calculate the daily internal alterations within a segment and then physically move material around (Appendix C).

2.5.1 Phytoplankton

The phytoplankton growth term is based on the maximum rate that can be achieved under optimal conditions. This maximum rate is then adjusted to account for environmental temperature, light, and nutrient conditions.

The function governing the effect of temperature on the process (equation B.1.1.1) is determined by the optimum and lethal temperatures of the species in question as well as the Q10 value (a measure of the slope of the linear, sub-optimum portion of the process-temperature curve). This construct was developed originally for terrestrial poikilotherms (Shugart et al., 1974) and modified for aquatic systems (Park et al., 1974). A detailed description of this temperature function and the coefficients that affect it can be found in Scavia and Park (1976).

After correction for non-optimal conditions as above, the growth rate must be adjusted to reflect the existing conditions of light and nutrients. These two variables are seldom optimal and therefore tend to reduce the maximum growth rate. The light reaching the photosynthesizing organism is a function of incoming solar radiation and light attenuation in the water column. This equation (U_l in B.1.1) has been used in many modeling efforts (e.g., DiToro et al., 1971; Scavia and Park, 1976; Canale et al., 1975). Nutrient limitation is a second factor reducing growth. As the phytoplankton grow, they gradually exhaust the limited pool of phosphorus and/or nitrogen available to them. Note that there are other necessary materials the organisms may require, such as silica, carbon, sulfur, vitamins, and trace metals; however, they are not modeled at this time. Nutrient limitation is handled by a hyperbolic function found to work well in enzyme kinetics and nutrient-based phytoplankton growth experiments (e.g., Dugdale, 1967; Eppley, Rogers, and McCarthy, 1969; McIssac and Dugdale, 1969). For phosphorus it takes the following form:

$$U_p = P/(P+K_p), \quad (2.5.1)$$

where K_p is the half-saturation constant, the phosphorus concentration at which the growth rate is half of the maximum. For nitrogen ($\text{NO}_3 + \text{NH}_3$) the reduction takes the form

$$U_n = \frac{\text{NO}_3 + \text{NH}_3}{\text{NO}_3 + \text{NH}_3 + K_n}, \quad (2.5.2)$$

where K_n is the half-saturation constant.

Various algorithms have been suggested for modeling the effects of limitation by more than one factor at a time. In some modeling efforts, a

multiplicative effect of limitation is assumed (DiToro et al., 1971; Canale et al., 1975; Goodall, 1975; Chen and Orlob, 1975) as follows:

$$U = U_1 * U_2 * U_3 * \dots , \quad (2.5.3)$$

where U_i is an individual limitation term. Others have suggested that the total effect is controlled by Liebig's law of the minimum (Larson, Mercier, and Malueq, 1973)

$$U = \text{Min} (U_1, U_2, U_3, \dots) . \quad (2.5.4)$$

More recently, an algorithm analogous to the harmonic mean used for electrical resistors in parallel has been suggested (Bloomfield et al., 1973; Scavia and Park, 1976); it is

$$U = N / \sum_{i=1}^N (1/U_i) , \quad (2.5.5)$$

where N is the number of limitation factors.

DiToro et al. (1971) had reasonable success when comparing observed phosphorus uptake rates at various nutrient concentrations in batch cultures (Ketchum, 1939) with those predicted by equation 2.5.3. Sykes (1974), however, suggests that the true effect of multiple limitation may not be observed in batch culture experiments. There have been few other investigations of a similar nature and one of the present authors (Scavia) has been equally successful in matching Ketchum's data to predictions with equation 2.5.4.

A recent study by Thomann et al. (1975) has attempted to compare the multiplicative and harmonic mean formulations. They varied the limitation construct, but otherwise used an identical model of the Lake Ontario ecosystem, and concluded (through comparing the simulation results) that the multiplicative formulation was to be preferred. This comparison, however, could have been biased, because the success of the constructs is determined by the values of U_i , which are in turn based on the choice of coefficient values (K_n, K_p). Given the range of actual values of the coefficients reported in the literature, sufficient variability is allowed such that, if the proper set of coefficient values is used, any of the three constructs discussed above can be used with satisfactory results. Thus, to base the construct selection on simulation results at this time is premature; further experimental evidence is needed.

We have decided to use the minimum function since it is most intuitively defensible for individual species and its effects are between those for the multiplicative and those for the harmonic mean construct.

The entire phytoplankton growth expression then is

$$G_p = G_{MAX}(T) \cdot \text{Min} \left\{ \frac{2.718F}{K_E} \cdot \left[e^{-\beta_1} - e^{-\beta_0} \right], U_p, U_n \right\} \cdot B, \quad (2.5.6)$$

where

- $G_{MAX}(T)$ = temperature-dependent maximum growth rate
- F = photoperiod
- K_E = extinction coefficient
= $K_{EX} + PHEPS \cdot B$
- $PHEPS$ = constant
- K_{EX} = extinction coefficient of pure water
- B = phytoplankton biomass
= $K_{EX} \cdot Z$
- β_1 = $\beta_0 \cdot e^{-K_{EX} \cdot Z}$
- β_0 = I/XIS
- I = incident light intensity
- XIS = saturating light intensity
- Z = depth.

Loss rates of phytoplankton are modeled to occur through respiration, grazing, and physiological death. The first rate term, respiration, is strictly temperature dependent in the model (equation B.1.3), although realistically there is probably some depth or light dependency involved. The rate can be species-specific for each of our four types of phytoplankton and is derived from an estimate of the maximum respiration rate at optimum temperature, the lethal temperature, and a rate term (equation B.1.1.1). The second phytoplankton loss rate term, grazing rate, is dependent on both temperature and phytoplankton biomass. This function is described fully in the zooplankton grazing section (equation 2.5.13 and B.2.1).

Rate of physiological death is modeled as a function of temperature and cell "health." Above a critical temperature (T_{MAX}), mortality rate increases exponentially as follows:

$$MORT = B2 \cdot e^{(T - T_{MAX})}, \quad T > T_{MAX},$$

where $B2$ is the maximum mortality rate below the critical temperature. At sublethal temperatures, mortality rate is modeled to be dependent on the physiological status of the cell. A first approximation relates cell "health" (and thus mortality rate) to the availability of nutrients and light

$$MORT = B2(1 - U),$$

where U is defined as the minimum of the individual limitation terms (equation 2.5.4). Thus, under healthy growing conditions, U approaches unity and MORT approaches zero. Poor growth conditions (U approaching zero) result in MORT nearing its maximum rate, B2.

During the cold winter months, cell metabolism is reduced and the requirements for light and nutrients are minimized. This acclimation to colder temperatures in nature would produce an overestimate of mortality in the model when light was limiting growth during the winter. To correct this, we have introduced the normalized temperature-growth relationship (TEMP) to the equation for sub-lethal temperatures

$$\text{MORT} = \text{B2} * \text{TEMP} * (1-\text{U}).$$

TEMP is low during the cold months and approaches unity during the summer (equation B.1.1.1). The general mortality rate equation is then

$$\text{MORT} = \begin{cases} \text{B2}(e^{\frac{\text{T}-\text{TMAX}}{\text{K}}}), & \text{T} > \text{TMAX} \\ \text{B2}(\text{TEMP}(1-\text{U})) & \text{T} < \text{TMAX}. \end{cases}$$

2.5.2 Zooplankton

The grazing term for each of the zooplankters in the model contains a species-specific, temperature-dependent grazing rate, GRAZ(T), multiplied by a reduction term following saturation kinetics based on food supply.

The temperature dependency of the grazing rate is similar to phytoplankton growth rate in that it operates at a maximum rate for optimal temperatures and decreases both above and below the optimum (equation B.1.1.1).

Each species of zooplankton is modeled as possessing the capability of displaying food preference following the approach of O'Neill (1969) and based on the experimental work of Bogdan and McNaught (1975), as well as other descriptive works (e.g., Hutchinson, 1967).

This grazing term is then corrected for ingestion efficiency and the defecated food becomes part of the detritus pool. The growth term is as follows:

$$G = \text{GRAZ}(T) * \frac{\sum_i B_i}{\sum_i B_i + K_{pp}} * B_Z * A, \quad (2.5.7)$$

where GRAZ(T) = temperature-dependent maximum grazing rate
 P_i = preference factor
 B_i = prey carbon
 K_{pp} = 1/2 saturation constant
 B_Z = zooplankton carbon
 A = ingestion efficiency.

This type of selective feeding has been used in other modeling efforts with varying degrees of success (O'Neill et al., 1972; Bloomfield et al., 1973; Canale et al., 1975; McNaught and Scavia, 1976).

In order to stabilize the phytoplankton-zooplankton interactions in the model in an ecologically sound manner, a minimum food level was introduced into the grazing equation. The feeding term above (equation 2.5.7) has been replaced by one which incorporates this relationship, and is derived as follows:

$$I = \frac{\sum P_i B_i - \text{MIN}}{\sum P_i B_i - \text{MIN} + K'_{pp}} \quad (2.5.8)$$

where MIN is the minimum food level necessary to stimulate feeding (McAllister, 1970; Parsons et al., 1969) and K'_{pp} is the new half-saturation constant. Since K_{pp} in equation 2.5.7 can be obtained from the literature (e.g., Richman, 1966) and K'_{pp} cannot, we must find a relationship between K_{pp} and K'_{pp} . One would require that

$$\frac{C}{C + K_{pp}} = \frac{C - \text{MIN}}{C - \text{MIN} + K'_{pp}}, \quad (2.5.9)$$

where $C = \sum P_i B_i$. For this to be true,

$$K'_{pp} = K_{pp} \left[\frac{C - \text{MIN}}{C} \right] = K_{pp} \left[\frac{\sum P_i B_i - \text{MIN}}{\sum P_i B_i} \right]. \quad (2.5.10)$$

When this consumption term is used to estimate the loss of one particular phytoplankton type (equation B.1.4), the numerator is no longer summed over all food and thus the term MIN must be partitioned. To do this, we calculate a weighted individual minimum term, $X\text{MIN}_i$, based on food preference and availability

$$X\text{MIN}_i = \left[\frac{P_i B_i}{\sum P_i B_i} \right] \text{MIN}. \quad (2.5.11)$$

This then eliminates the possibility of having four food sources slightly below MIN and therefore no growth (when actually the total food is greater than MIN). The zooplankton growth term then becomes

$$G_z = \text{GRAZ}(T) * \frac{\sum_i (P_i B_i - X\text{MIN}_i)}{\sum_i (P_i B_i - X\text{MIN}_i) + K'_{pp}} * B_z * A \quad (2.5.12)$$

and the individual phytoplankton loss term due to grazing is

$$G_z = \text{GRAZ}(T) * \frac{P_i B_i - X\text{MIN}_i}{\sum_i (P_i B_i - X\text{MIN}_i) + K'_{pp}} * B_z \quad (2.5.13)$$

A form of this construct was originally suggested by Bloomfield et al. (1973); however, if one is to use information from the literature for MIN and K_{pp} , the weighting functions described above must be included.

The loss of zooplankton is modeled to occur through metabolic respiration, physiological death, and grazing by higher trophic levels. Since fish are not explicitly included in this model, higher trophic level grazing, other than the carnivorous zooplankton group, is incorporated in a single term linearly proportional to zooplankton density (equation B.2.5). Respiration is a species-specific temperature function (equation B.2.2). Physiological death is considered minimal (≈ 4 percent per day; Hall, 1964) under normal conditions, and is modeled to increase exponentially above critical or lethal temperatures (equation B.2.4).

2.5.3 Detritus

The detritus component is modeled as non-living, particulate organic carbon. The pool increases as the phytoplankton and zooplankton die and as the zooplankton defecate. Losses from the pool are through zooplankton grazing and bacterial-induced decay (assumed first order) to inorganic carbon (equation B.7.3).

2.5.4 Phosphorus

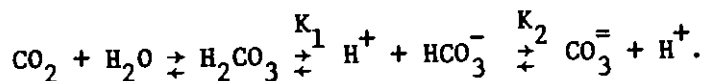
During phytoplankton growth, phosphorus is removed from the aqueous phase and incorporated into the cell. In the model this is handled stoichiometrically; that is, the phosphorus uptake is equal to the P:C ratio times the carbon uptake. Phosphorus is returned to the system as respiratory by-products of each of the biological components and through decay of detrital material by similar stoichiometry. No time-lag is included between the release of phosphorus from living and dead particles and its entry into the pool available for uptake by phytoplankton.

2.5.5 Nitrogen

During most of the accelerated growth phase, phosphorus appears to be the major limiting nutrient for growth in Lake Ontario. However, during a portion of this phase, nitrogen could become at least as important. The uptake of nitrogen is also stoichiometric, based on an N:C ratio. The model does consider a time-lag between release of nitrogen by organisms and its subsequent reuse. This is handled by forming three nitrogenous components: dissolved organic nitrogen, ammonia, and nitrate. Material enters the dissolved organic nitrogen pool through excretion and detrital decay, is converted to ammonia, and is finally oxidized to nitrate, which is the primary nitrogen form in Lake Ontario. Both ammonia and nitrate are utilized by the autotrophs.

2.5.6 Inorganic Carbon

An investigation of the total inorganic carbon system (TCO_2) has been included in the model. The description of and equations relating to the species of inorganic carbon have been well documented under equilibrium conditions (Stumm and Morgan, 1970). Basically, the system consists of the hydration of CO_2 and its accompanying dissociation into ionic forms as follows:



The first step above is rate controlling, with ion formation being instantaneous in the context of our time frame.

The first and second dissociation constants (K_1 , K_2), which control the ionic concentrations under equilibrium, are functions of temperature and ionic strength. Those used in this model are taken from Stumm and Morgan (1970) and have been corrected for the mean ionic strength of Lake Ontario. CO_2 solubility is temperature dependent and the values were extracted from the same reference. From the above constants and a knowledge of any pair of carbon parameters (TCO_2 , Alk, pCO_2 , pH), the equilibrium distribution of ionic forms can be calculated.

In the model, the simplifying assumption of constant alkalinity has been made; this neglects changes due to carbonate kinetics and remineralization reactions. The total inorganic carbon is followed through the biological system (equation B.7), with the sources being through community respiration and remineralization and the removal being by phytoplankton uptake. At the end of each day the system is brought back toward equilibrium through gaseous exchange (Gasx) across the air/water interface, utilizing a model based on the work of Kanwisher (1963) and Liss (1973)

$$\text{Gasx (moles/cm}^2\text{/sec)} = 2.78 \times 10^{-7} * (0.03 * \text{WIND}^2 + 2)$$

$$* \text{ALPHA} * (\text{PCO}_2 - 0.00033),$$

where the partial pressure of atmospheric CO_2 (PCO_2) is assumed constant at 330 ppm, WIND is wind speed at 10 cm over the water (See Section 2.3), and ALPHA is the solubility of CO_2 .

Since the rate controlling hydration of CO_2 is slower than the biological perturbations to the system, the distribution of carbon species is continually removed from equilibrium.

The equations describing the inorganic carbon species distribution with known TCO_2 and alkalinity were adopted from Park (1969)

$$X = (C-A) + \frac{\left[AK - CK - 4A + \sqrt{(4A + CK - AK)^2 + 4(K-4)A^2} \right]}{2(K-4)}$$

$$Y = \frac{CK - \sqrt{(4A + CK - AK)^2 + 4(K-4)A^2}}{K-4}$$

$$Z = \frac{AK - CK - 4A + \sqrt{(4A + CK - AK)^2 + 4(K-4)A^2}}{2(K-4)}$$

where

$X = \text{H}_2\text{CO}_3$ (assumed all CO_2)

$A =$ carbonate alkalinity ($\text{HCO}_3^- + 2\text{CO}_3^{=}$)

$C =$ total inorganic carbon ($\text{H}_2\text{CO}_3 + \text{HCO}_3^- + \text{CO}_3^{=}$)

$K = K_1/K_2$

$Y = \text{HCO}_3^-$

$Z = \text{CO}_3^{=}$

2.5.7 Sediment/Benthic Fauna

This final component of the modeled system is treated apart from the simultaneous dynamic system equations described above since little is known of the dynamics of the Lake Ontario benthos. Jonnassen (1972) detailed the dynamics of chironomid larvae in Lake Estrom, and Zahorcak (1974) has proposed a model of their dynamics. Similar studies have been made in other ecosystems, but the dynamics of Pontoporeia, the dominant form in the Lake Ontario benthos, are not clear.

It was decided to use a more empirical approach to model the benthic system since available data from Lake Ontario (Johnson and Brinkhurst, 1971a, b, c) warrant it. At the end of each integration step (1 day) of the simultaneous differential equations (Appendix B), the influx of particulate organic carbon to the sediment is calculated (Section 2.4). Approximately 9 percent of this sedimentary carbon is lost to the deep sediments, and of the 91 percent left, 41 percent is lost to microbenthic metabolism

(Johnson and Brinkhurst, 1971c.), so the amount of sedimentary carbon available to the macrobenthic community is 54 percent of that falling to the bottom or

$$SED_m = SED_{m-1} + 0.54 * RAIN. \quad (2.5.16)$$

In Johnson and Brinkhurst's second paper (1971b), annual growth rates and daily respiration rates were evaluated as functions of temperature

$$\text{Growth rate} = G = \frac{T^2}{10} \text{ (year}^{-1}\text{)}.$$

$$\text{Respiration rate} = R = \text{EXP}[1.5 + 0.14T - 0.34 \ln W] \text{ (}\mu\text{g-O}_2\text{/mg/day),}$$

where T = temperature ($^{\circ}\text{C}$)
 W = ash-free weight ≈ 1.98 mg.

The growth expression was converted to a daily rate and respiration was converted to mg-C/mg-C/day, resulting in

$$\text{GROW} = \frac{T^2}{3650} \quad (2.5.17)$$

$$\text{RESP} = 0.0017e^{0.14T}. \quad (2.5.18)$$

The change in available sediment due to macrobenthos growth and respiration is calculated as follows:

$$SED = SED - (\text{GROW} + \text{RESP}) * \text{BEN}, \quad (2.5.19)$$

where BEN is macrobenthos carbon. If SED does not become negative, the new benthic carbon is calculated as

$$BEN_m = BEN_{m-1} + \text{GROW}. \quad (2.5.20)$$

If SED does become negative, however, at least part of the increase in benthic carbon at that temperature (GROW) is not possible. A new value for SED is then calculated as

$$SED = SED - \text{RESP}, \quad (2.5.21)$$

which requires the benthos respiratory requirements to be met first. If SED is now positive, it is assumed that this value can be utilized for benthos growth

$$BEN_m = BEN_{m-1} + SED \quad (2.5.22)$$

and there is no available sediment (SED) at the start of the next time step. If SED is still negative in equation (2.5.21), the metabolic needs of the benthos at that temperature cannot be met through respiration of ingested food, and endogenous respiration will have to account for a portion of its needs. The metabolic needs satisfied by the food, R' , is equal to the amount of food available, SED. The endogenous portion, R'' , will be the benthic animals' total need minus that satisfied through ingestion or

$$R'' = RESP - R'. \quad (2.5.23)$$

The loss due to endogenous respiration is then subtracted from the existing benthic carbon (obviously no growth occurs)

$$BEN_m = BEN_{m-1} - R'', \quad (2.5.24)$$

and there is no accumulation of available sediment during this time-step. A concise flow chart of the logic is presented in figure 6.

3. PRELIMINARY EVALUATION

Evaluation of large-scale, non-linear ecosystem models has been largely qualitative. Little work has been done to develop robust tests for accuracy in prediction. To date, most work has been evaluated by comparing predicted and measured concentrations of biological and chemical variables. We shall do the same, but shall also include a secondary level of evaluation.

Predicted concentrations are determined by solving the simultaneous differential equations of the system (Appendix B). It is probable that these solutions are not unique and thus "correct" predictions could be obtained, though based on incorrect mechanisms or coefficients. One way to investigate whether this is occurring is to compare observed data with predictions at the process level (i.e., verify the terms in the simultaneous equations). If one can verify some of these processes, the state variable predictions (Section 3.2) are on a firmer base.

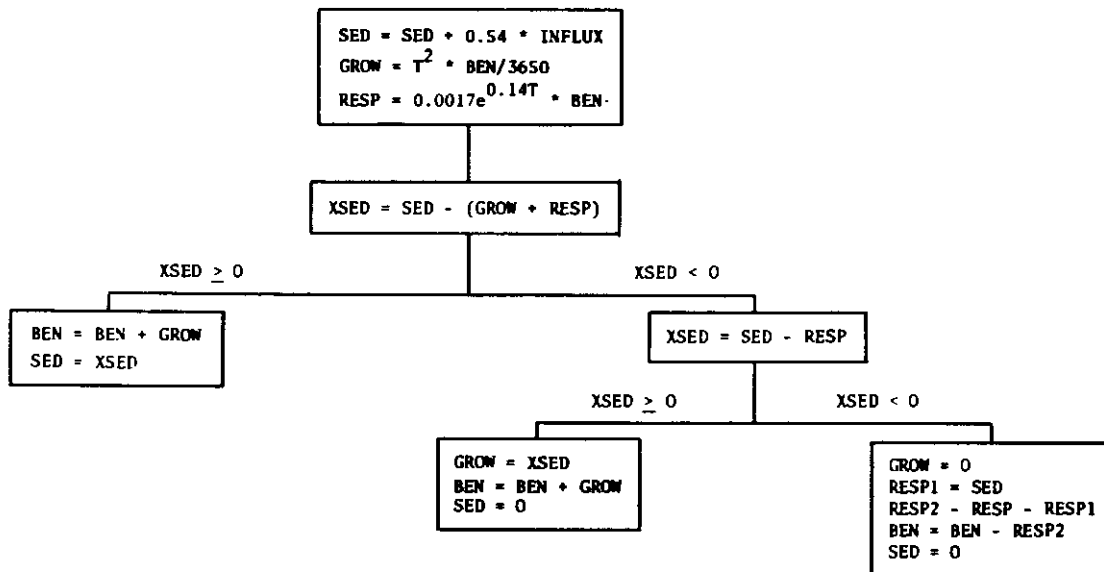


Figure 6. Logic of benthic carbon calculations (see text for definition of terms).

3.1 Process Simulation

Although the data necessary for detailed comparisons on the process level are much more difficult to obtain, a few studies have produced results that can be used for this purpose.

Primary production is the foundation of any food web model. Both nutrient concentrations and animal standing crops are highly coupled to the phytoplankton compartment, which is in turn driven by primary production. Glooschenko et al. (1974) found that production in Lake Ontario varied between 0.15₂ and 1.08 g-C/m²/day, and they estimated total production to be 170 g-C/m² between April and December 1970. Stadleman et al. (1974) measured production rates between 0.058 and 1.24 g-C/m²/day offshore and 0.173 to 1.85₂ g-C/m²/day inshore. Simulation results vary between 0.01 and 1.2 g₂-C/m²/day with an integrated value between April and December of 180 g-C/m² (fig. 7a). Glooschenko et al. (1974) also estimated assimilation numbers (mg-C/Chla/hr). For the comparison in fig. 7b we used equation 2.3.1 (to obtain the number of sunlit hours per day) and a carbon to chlorophyll a ratio of 50 to get mg/mg/day. Stadleman et al. (1974) also measured production in mg-C/mg Chla/day and found a range of 3.4-17.8. Again we used a C:Chla ratio of 50 and simulated a range of 2.0-21.0.

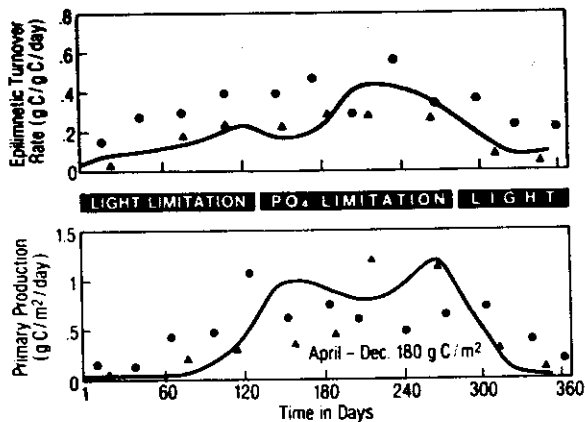


Figure 7. Predicted and observed primary production (a. lower) and epilimnetic turnover rate (b. upper). Circles are data from Glooschenko et al. (1974) and triangles are data from Stadlerman et al. (1974).

It is also interesting to examine the ratio of primary production (P) to total community respiration (R) (fig. 8). The P:R ratio reaches 7 in the early spring and approaches the compensation point (P:R = 1) during mid-summer and winter in the epilimnion. The P:R ratio in the thermocline region reaches unity during mid-summer. Although the physical segmentation of the model (i.e., three aggregate vertical zones) does not allow a precise prediction of the compensation depth, it does indicate that it occurs within the lower epilimnion-upper thermocline region. Vertical distributions of chlorophyll a concentration (Stoermer et al., 1974) support this.

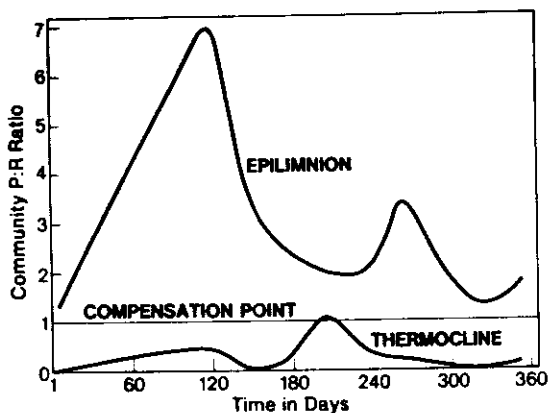


Figure 8. Predicted community production: respiration ratios for epilimnion and thermocline segments.

Sedimentation is an important phenomenon in lake ecosystems. Simulation results show an overall range of sedimentation rate from 0.0004 m/day for small non-diatoms in the epilimnion (mid-April) to 2.9 m/day for large diatoms in the hypolimnion (early November). The ranges of individual predicted sinking rates are presented in table 1. The maximum rates are well within the range reported in a review of marine diatom sinking by Smayda (1970) and *in situ* measurements for Lake Ontario (Burns and Pashley, 1974). The very low minimum sinking rates suggest the algae are approaching a positive buoyancy when actively growing (April), and at least one study (Smayda and Boleyn, 1966a) has indeed reported a marine diatom rising during illuminated experiments.

Table 1. Predicted Sinking Rates

		Small Diatoms		Large Diatoms		Small Non-Diatoms		Large Non-Diatoms		Detritus	
		Min	Max	Min	Max	Min	Max	Min	Max	Min	Max
Epilimnion	Rate (m/day)	0.0005	0.0027	0.008	0.041	0.0004	0.0018	0.006	0.031	0.67	1.15
	Date	112	168	112	168	112	168	112	168	56	224
Hypolimnion	Rate (m/day)	0.09	0.20	1.4	2.9	0.06	0.13	1.03	2.2	0.69	0.76
	Date	196	308	196	308	196	308	196	308	84	336

Phytoplankters sink both as living cells and as detritus after death, but the predicted sinking rates of detrital material are generally higher than those of living cells. This is consistent with Smayda's (1974) experimental work on freshwater diatoms, in which dead cells were observed to sink 1.2-3.8 times faster than live cells.

Loss of particulate matter to the sediments provides food for benthic organisms; and although no provision is made for regeneration of dissolved inorganic nutrients from the sediments in the model at this time, the particulate matter serves as a potential source for this process. Johnson and Brinkhurst (1971c) report total sedimentary input rate at a nearshore station in Lake Ontario to vary between 0.05 and 0.3 g dry solids/m²/day (their fig. 3). They also report organic matter as contributing 32 percent of the total input, or 0.016-0.1 g-C/m²/day. One would expect sedimentation to fluctuate more near shore than in the open water; however, Johnson and Brinkhurst's (1971c) measurements are an indication of daily sedimentary input rates for the lake. The simulated influx rate (0.03-0.12 g-C/m²/day)

agrees quite well and when divided into portions attributed to detrital and phytoplankton sinking indicates that other than during the spring, the bulk of the material entering the sediment is dead. This will be important for driving improved benthic animal and microflora models as it is a measure of the "value" of the incoming food.

3.2 State Variable Simulation

The ultimate goal of any model developed for management purposes is to predict the concentrations of particular substances. In building a model designed for both research and eventual application in a management context, testing on the process level usually has its payoff in the prediction of the state variables. While we are not solely interested in the precision of these predictions at this stage of development, the predictions should show reasonable agreement with observed data. Where this is not possible, further investigations into the accuracy of the process descriptions and coefficient values are needed. Process constructs have been previously discussed (Section 2 and Appendix B) and the values of the coefficients used in this calibration, as well as the derivation of these coefficients, are discussed in Appendix A.

Observations are available for chlorophyll *a*, crustacean carbon, available phosphorus, Kjeldahl nitrogen (organic + ammonia), nitrate, and ammonia. Also, data is available for pH, alkalinity, and, by calculation, other parameters in the carbonate system. Data used for the epilimnion (fig. 9 and 10) and hypolimnion (fig. 11) are from observations compiled by Thomann et al. (1975). The observed data in figures 9 and 10 are lakewide average concentrations for 0-17 m, whereas the modeled epilimnetic depth is calculated dynamically and varies between 12 and 36 m. Observed data in figure 11 are lake-wide averages for below 50 m, and the predicted top of the hypolimnion is between 20 and 45 m.

Phytoplankton carbon (C:Chl *a* = 50) is predicted quite well. Spring and fall peaks as well as the mid-summer trough, are simulated. Zoo-plankton carbon is predicted within the reported range, and the nitrogen system compartments are predicted well, with the exception of an underestimate of the Kjeldahl portion. Simulated organic nitrogen considers only the dissolved organic fraction whereas Kjeldahl nitrogen represents both particulate and dissolved organic fractions. If detrital carbon is converted to organic nitrogen stoichiometrically (C:N = 0.18) and added to the dissolved organic and ammonia pool, a more accurate prediction results (about 0.22 mg-N/l during July). Depletion of available phosphorus during spring and summer is simulated well, and nutrient predictions in the hypolimnetic waters (fig. 11) are all quite good. The simulation of the hydrogen ion activity (pH) agrees well with surface data from the IFYGL program (fig. 12) until late summer, when the model estimates become too high. Analysis of rates of CO₂ generation and loss shows this is due to the second phytoplankton peak. The gaseous exchange response (fig. 13) also shows the anomaly late in the year in response to the higher pH.

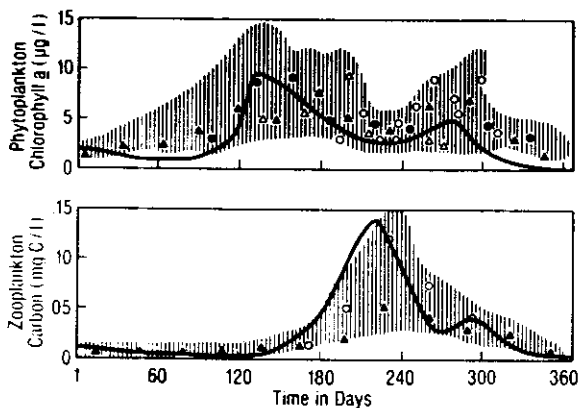


Figure 9. Predicted and observed epilimnion state variables. Curve is prediction and shaded area represents lake-wide mean ± 1 standard deviation. 1967 - open circles, 1969 - closed circles, 1968 - open triangles, 1970 - closed triangles.

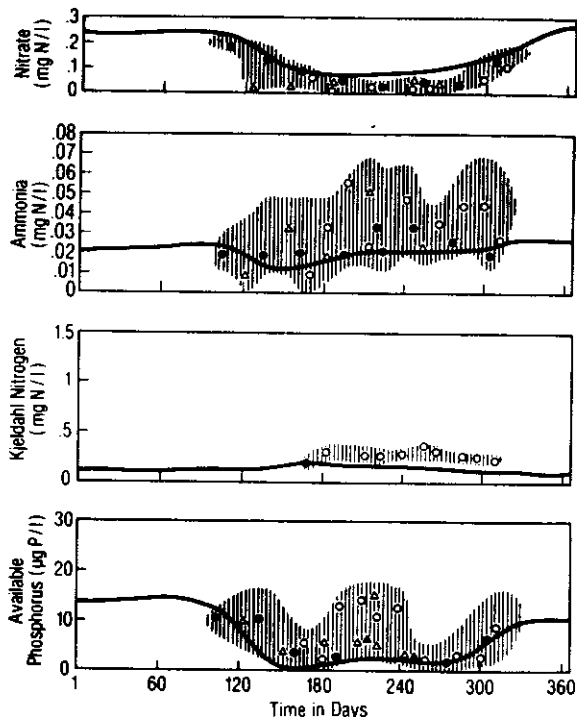


Figure 10. Predicted and observed epilimnion state variables (see figure 9.).

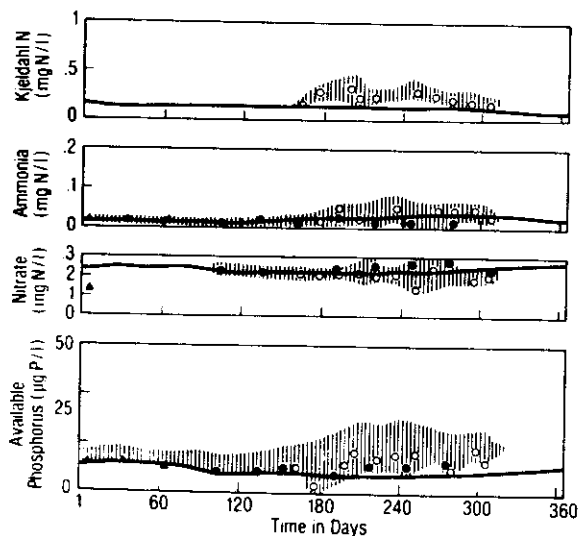


Figure 11. Predicted and observed hypolimnion state variables (see figure 9.).

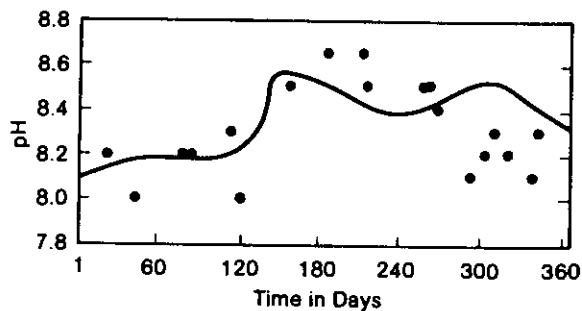


Figure 12. Predicted (curve) and observed (dots) pH.

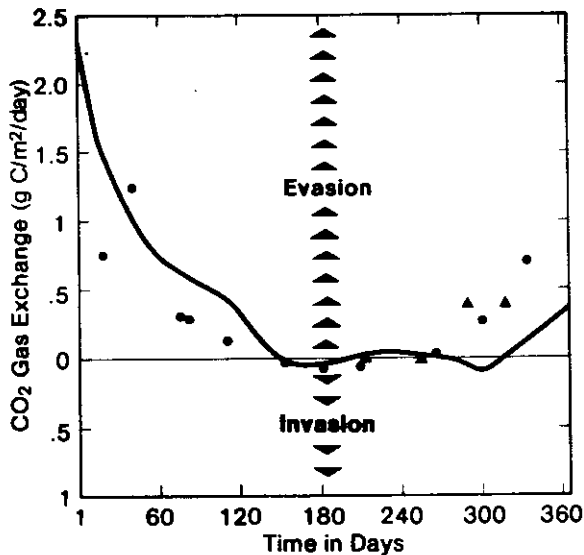


Figure 13. Predicted (curve) and observed (Eadie and Robertson, 1976) CO_2 gas exchange.

4. ANALYSIS OF MODEL OUTPUT

The interrelationships among various modeled phenomena can offer interesting theories involving the relative importance of the processes within this aquatic ecosystem.

Simulation results are plotted and examined for general patterns of trophic level succession (fig. 14). Bimodal curves of total phytoplankton carbon and total zooplankton carbon, as well as signs of nutrient depletion beginning in late spring and lasting throughout summer are evident. The bimodal phytoplankton curve seems characteristic of Lake Ontario based on 4 years of chlorophyll *a* data compiled by Thomann et al. (1975); however, the bimodal zooplankton population prediction may not be typical. Patalas (1969) observed a minor second peak in crustacean zooplankton carbon in 1967, but others have not (e.g., Watson and Carpenter, 1974).

The general relationships between the curves in figure 14 suggest that the phytoplankton standing crop is jointly regulated by the nutrient concentrations and zooplankton standing crop, as might be expected.

The dynamics of the nitrogen system (organic N-NH₃-NO₃) are shown in figure 15. The buildup of detritus and organic nitrogen following the spring phytoplankton peak appears to be an important source of replenishment of the inorganic supply (predominantly nitrate).

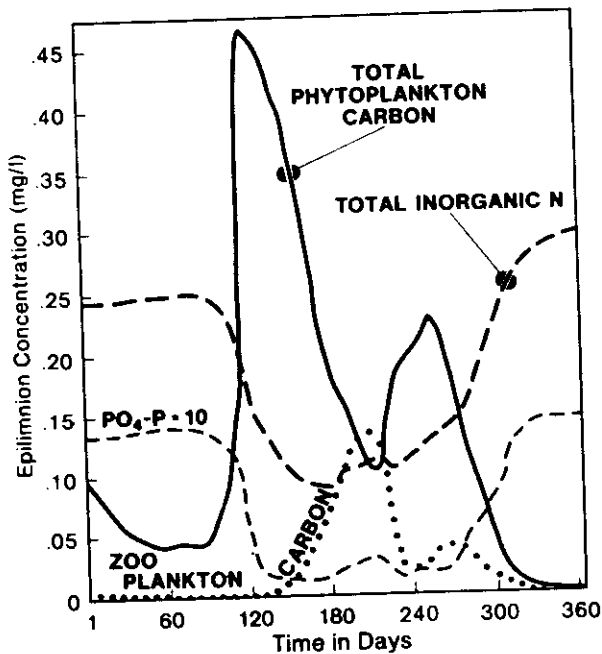


Figure 14. Simulated epilimnetic state variable dynamics.

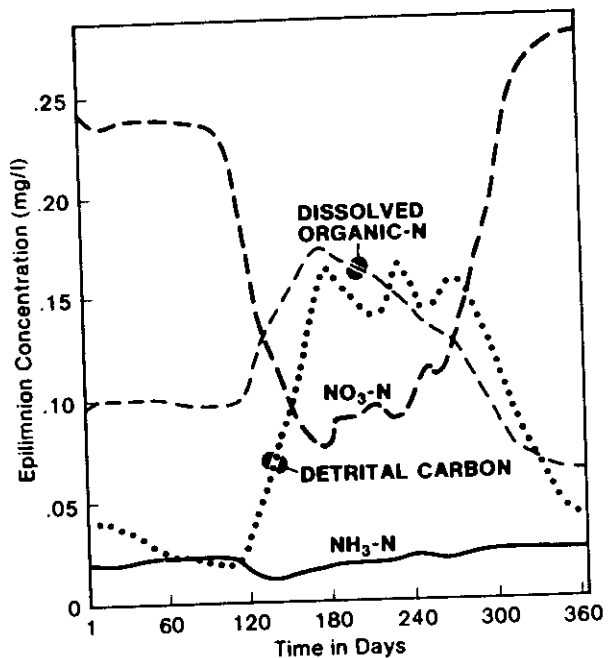


Figure 15. Simulated dynamics of the epilimnetic nitrogen system. Detrital carbon is an indication of particulate organic nitrogen.

Although we are not interested in individual phytoplankton groups at this stage of model development, the succession of these groups is interesting and will be necessary for developing eutrophication models in the future. The only group-specific differences for the phytoplankton in these simulations are in the sinking and grazing terms (see Sections 2.4 and 2.5.2); all other phytoplankton processes were parameterized equally for all groups. There was a general succession from small forms to large (fig. 16); for the two groups of small phytoplankton, the differences between the sinking rates (table 1) and the grazing pressures (table A.2) seem to have been balanced, although the effect of dissimilar sinking seems very important in segregating the two large forms. It is also interesting to note that the bimodal curve for total phytoplankton (fig. 14) actually represents the combination of the curves for the four general groups.

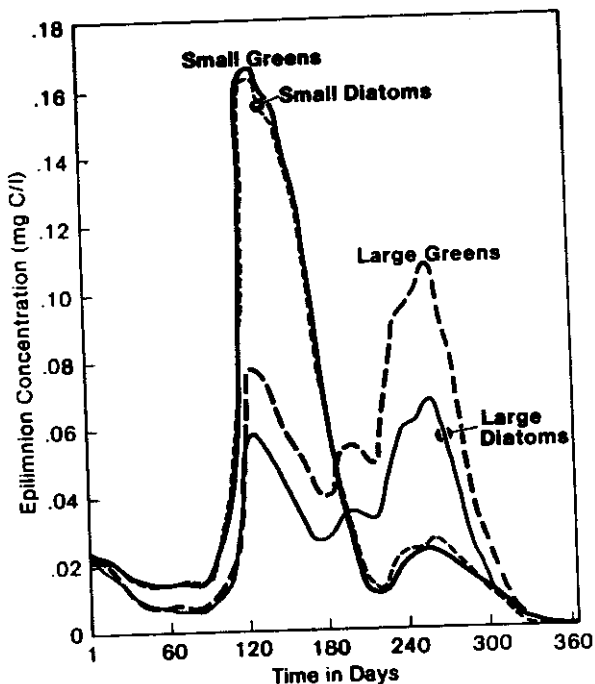


Figure 16. Simulated succession of epilimnion phytoplankton groups.

The individual plots of the zooplankton groups (fig. 17) are complex. The carnivorous zooplankton group follows the herbivorous groups in succession, while large cladocerans and herbivorous copepods dominate early. The latter two groups are probably preyed upon by the carnivorous zooplankton only during the early life stages in nature and therefore experience less predatory pressure than the rotifers, which are thought to receive continual heavy predation. In addition to the above groups, the mysids, a cold water herbivore, are modeled. Simulation results show mysids dominate the zooplankton in the hypolimnion because of being able to outcompete the other groups at lower temperatures (i.e., lower values for TOPT and TMAX).

Concentrations of the state variables are dependent upon the relationships among the processes that contribute to their dynamics. Simulated available phosphorus is determined by plant and animal excretion, remineralization, phytoplankton uptake, and diffusion. In our model, phytoplankton uptake is by far the most important process (fig. 18). In the epilimnion, diffusion and excretion are the main inputs balancing the loss due to uptake, while remineralization seems to play a more minor role. Nitrate concentration is controlled primarily by the interaction between the loss due to phytoplankton uptake and diffusion input to the epilimnion (fig. 19), although nitrification also contributes somewhat to the nitrate pool. The balance between phytoplankton uptake and diffusion into the epilimnion also accounts

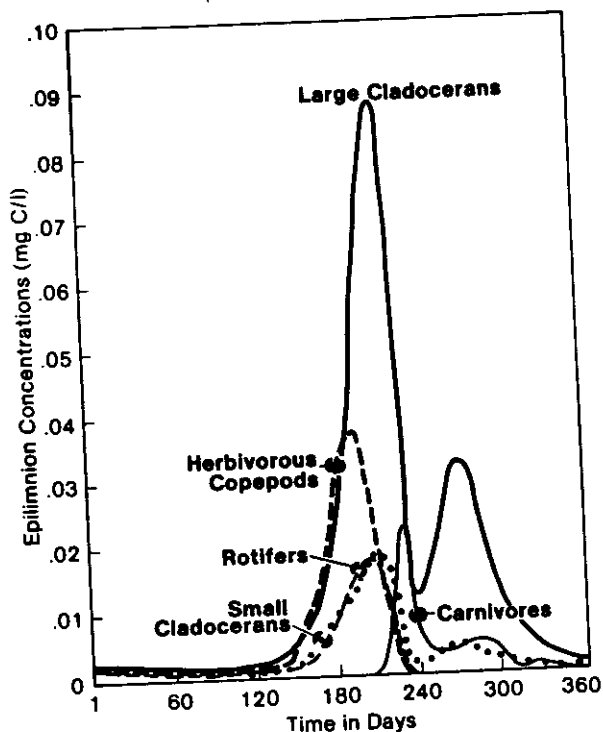


Figure 17. Simulated succession of epilimnion zooplankton groups.

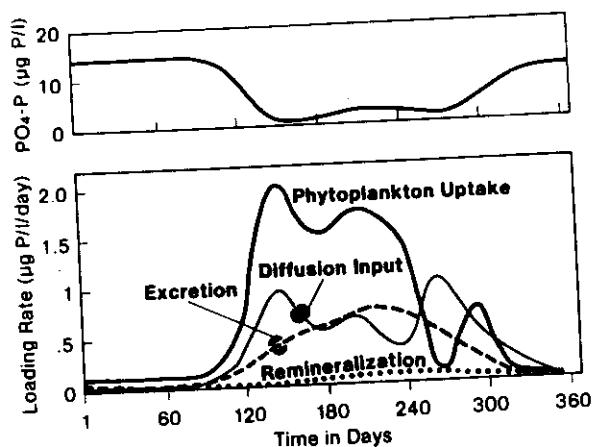


Figure 18. Simulated PO_4 concentration (upper) and seasonal dynamics of factors affecting PO_4 (lower).

for most of the variation in ammonia concentration; ammonification and nitrification contribute to a lesser degree. The inputs to the organic nitrogen pool are from plant and animal excretion and decay of detrital matter. Losses are due to ammonification and diffusion. Diffusion and excretion are the most important processes in this simulation of organic nitrogen.

The bimodal population curve of the large cladocerans (fig. 20) is controlled mainly by the interaction between consumption, respiration, and predation, with respiration being the most important loss. Further refinement of the higher trophic levels (including the addition of fish) will aid in better descriptions of the zooplankton dynamics.

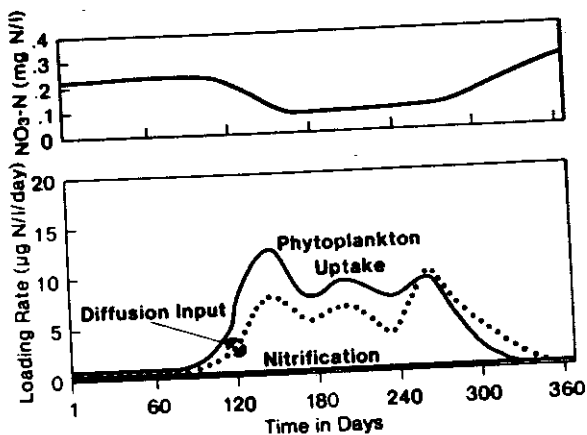


Figure 19. Simulated NO_3 concentration (upper) and seasonal dynamics of factors affecting NO_3 (lower).

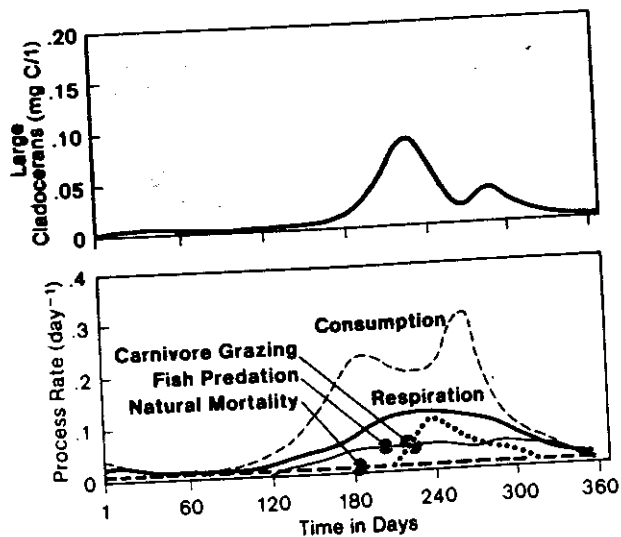


Figure 20. Simulated large cladoceran concentration (upper) and seasonal dynamics of factors affecting large cladocerans (lower).

The dynamics of the small diatoms (fig. 21) are controlled largely by primary production (photosynthesis) and grazing, with respiration and non-grazing mortality less important. The loss rate due to sinking out of the epilimnion is very small for this group. A maximum rate of 0.0027 m/day was calculated, representing an instantaneous loss of 0.00015/day from the epilimnion. Diffusion effects seem important for this small algal group, since this loss rate is simulated to be at least as important as respiration during parts of the year. The various limitation effects, as well as the overall temperature reduction, indicate that light limitation occurs during the winter and early spring and phosphorus becomes limiting in the spring and late summer. The effect of temperature results in the general, overall sinusoidal shape of the production curve (see Section 3.1).

Figure 22 shows the overall sediment accumulation (29 g-C/m^2) and how it is partitioned throughout the year. On an annual basis, 42 percent and 38 percent of the sedimentary carbon is lost to macrobenthic and microbenthic respiration, respectively. In this simulation, 9 percent becomes unavailable and 11 percent is contributed to macrobenthic production.

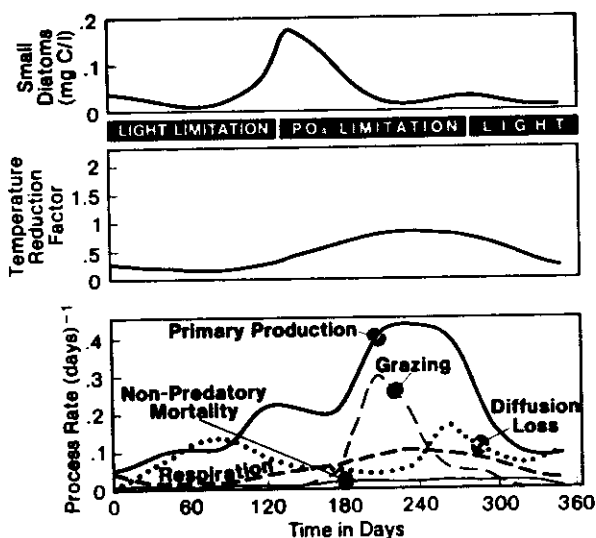


Figure 21. Simulated small diatom concentration (upper); nutrient, light, and temperature limitation (middle); and seasonal dynamics of factors affecting small diatoms (lower).

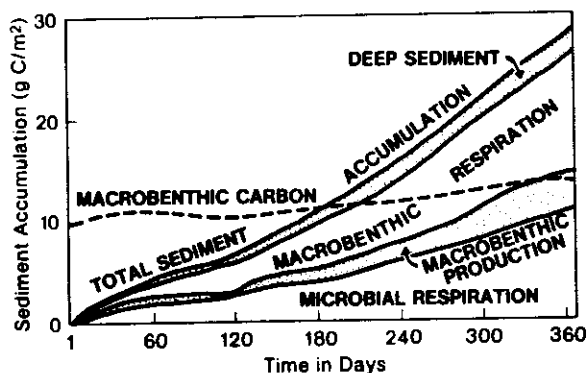


Figure 22. Accumulation and partitioning of sediment carbon and seasonal dynamics of the macrobenthos.

The benthic carbon compartment increased by 3.4 g-C/m^2 over the year, although in reality one would expect the annual change to be close to zero. We have used only a gross approximation to simulate the macrobenthic community by not including important processes, such as fish predation or sensitivity to dissolved oxygen. A more complete model would probably conform to our expectations more closely.

5. ANALYSIS OF MODEL FUNCTIONS

By examining the effects of specific alterations in the model, one can examine the relative importance of various modeled processes. This analysis can aid in verifying or rejecting portions of the model and can assist in making decisions concerning the required level of model complexity. By comparing the results of simulations before and after the alterations with what one might expect from real-life situations, the constructs can be evaluated individually.

5.1 Diffusion

In our basic model, the vertical diffusion of phytoplankton, detritus, and nutrients is controlled by calculated diffusion coefficients and concentration gradients. To explore the significance of diffusion, the model was altered by eliminating this process while keeping sedimentation active. This alteration results in a very early spring phytoplankton peak and subsequent nutrient depletion. Also, through sedimentation and the lack of epilimnetic nutrient replenishment, the phytoplankton does not form a second peak, the zooplankton does not reach normal density, and available phosphorus does not increase in the fall as would be expected. At the same time, hypolimnetic nutrient concentrations continually increase rather than remain relatively stable (fig. 11) as before.

The earlier phytoplankton peak can be attributed to the absence of diffusion in the following way. In the original simulation, phytoplankters diffuse out of the epilimnion rapidly before and after stratification (fig. 21). In this situation, the phytoplankton increases through photosynthetic growth and then decreases through sedimentation before the zooplankton respond.

Regeneration of available phosphorus in the original simulation occurs primarily through diffusion and excretion (fig. 18). With diffusion shut off and excretion reduced considerably through the reduction of zooplankton populations, there is essentially no replenishment of the epilimnion phosphorus.

The major loss term for organic nitrogen in the original simulation is diffusion. With no diffusion, epilimnetic organic nitrogen increases by a factor of 1.5, stimulating regeneration of the nitrate concentrations within the epilimnion without diffusion.

It is apparent that the ecosystem dynamics are heavily dependent on diffusion since this process supplies most of the epilimnetic phosphorus after the breakdown of stratification and also controls an important part of the loss of phytoplankton.

5.2 Sedimentation

Sedimentation is critical for the support of benthic life. As discussed in Section 4, approximately 29 g-C/m^2 is deposited into the sediment during a 1-year simulation, enough material to increase the benthic carbon from 10 to 13.4 g/m^2 (or 34 percent). To consider the influence of sedimentation on both the benthic and pelagic communities, a simulation was run with all conditions the same as the basic model, except that sinking was eliminated.

The most dramatic influence was seen in the case of benthic carbon, reducing it by 65 percent ($10-3.5 \text{ g-C/m}^2$) during 1 year. In reality, one would expect all benthic animals to die without food, reducing the living biomass by 100 percent. In this crude representation of the benthic system, the distinction between live and dead biomass is vague and surely the benthic

organisms would die before respiring all of their body carbon. With the omission of fish predation at this time, the only loss of benthos is through respiration. The inclusion of predatory losses would aid in better simulation of the benthic organisms. It is obvious, still, that sedimentation is necessary to drive benthic production.

Alterations in the pelagic community were also observed. The first phytoplankton peak increased slightly, the second peak increased by 30 percent, and epilimnetic detritus doubled. The system was stabilized, however, by increased grazing, producing a zooplankton concentration twice that obtained in the original run (0.26 mg-C/l).

The effect of sedimentation on the water column is not as great as that of diffusion; however, it does have considerable impact on the system.

5.3 Self-Shading

The model uses a linear relationship between the extinction coefficient and phytoplankton carbon (ϵ' in equation B.1.1). To examine the impact of self-shading, we eliminated the plankton-related term from the equation. This reduces the total extinction coefficient to a constant, i.e., the extinction coefficient for water alone.

With this alteration, there was very little change in the simulation results. When self-shading should have influenced primary production, phosphorus limitation was dominant. When phosphorus became less limiting, and light began to limit, the algal concentration was relatively low. The slightly reduced early light-limitation resulted in slightly higher algal concentrations, which led to lower phosphorus during the summer. This resulted in a slightly lower fall phytoplankton peak.

Although self-shading did not appear to be very important in this particular case, this result should not be generalized. It may have just been coincidental that in this situation light-limitation was balanced by phosphorus limitation.

5.4 Fish Predation

When fish predation was eliminated from the model, maximum zooplankton carbon increased by 86 percent, a concentration far greater than observed. To obtain realistic results, the fish predation term is necessary. Since the true value of this predation term is undoubtedly not a constant, the model representation (equation B.2.5) is a gross simplification. To be able to accurately estimate fish predation, models attempting to follow the dynamics of the fish populations will be necessary.

5.5 Temperature

Temperature is one of the very basic driving forces, both in the model and in the real world. With a year-round temperature increase of 5° C, the model predicted a general shift in the peaks of all state variable curves. The phytoplankton spring bloom shifted from mid-May to late April, and this caused a shift of the zooplankton maximum from early-August to mid-June. Temperature variations do have a significant effect on the magnitude of this model's predictions, but interesting effects will also be manifest in examining seasonal species succession. The succession of zooplankton and phytoplankton groups due to temperature changes will be explored after the model has been verified for the separate plankton groups.

6. SUMMARY

A one-dimensional model of the Lake Ontario ecosystem has been developed to describe the more important biological and chemical processes within the Lake Ontario ecosystem.

A physical model, driven by surface temperature and wind velocity, predicts temperature profiles, turbulent vertical diffusivity coefficients, and variations in layer thicknesses (epilimnion, thermocline, and hypolimnion). The predictions have been verified through comparisons with actual measurements of temperature and thermocline depth.

An original formulation is used to calculate rates of particle sinking. The construct, based on Stokes' law, form corrections, and the physiological health of the phytoplankton, results in reasonable sinking rates for individual species as well as for total influx to the sediment.

The biological compartments of the model contain state-of-the-art constructs, some developed as part of this effort, others adapted or modified from other modeling projects. The model follows the cycle of carbon through phytoplankton, herbivorous and carnivorous zooplankton, detritus, macrobenthos, and inorganic species. Nitrogen cycling is initiated stoichiometrically and then continued through organic nitrogen, ammonia, and nitrate phases. Phosphorus is handled stoichiometrically.

A new construct for modeling phytoplankton mortality was developed, relating non-grazing mortality to the physiological health of the algae as determined by light and nutrient limitation. An important modification of an existing zooplankton consumption formulation is derived in order to relate measurable parameters to model coefficients. Also, an original formulation, based on temperature dependent growth and respiration requirements, is developed to describe the dynamics of the macrobenthos.

Preliminary evaluation indicates the model behaves in accordance with theoretical expectations. Detailed studies of the relationships between process phenomena and standing crop estimates also indicate general consistency of the model with basic ecological theory.

The accuracy with which the model predicts various process rates lends credence to the state variable estimates. Comparisons between predicted and observed rates of primary production, turnover, community P:R ratios, and sedimentation were favorable. Predictions of the concentrations of chlorophyll a, zooplankton carbon, available phosphorus, Kjeldahl nitrogen, ammonia, nitrate, pH, and CO₂ gas exchange were all consistent with observed values for the period 1967-1971.

Sensitivity of the model to diffusion, sedimentation, self-shading, fish predation, and temperature was investigated. Diffusion appears to be responsible for much of the epilimnetic phosphorus after stratification. In addition to being very important to the benthic community, sedimentation was also found to be important in accurately predicting biological and chemical dynamics within the water column. Self-shading was not important when compared with the effect of phosphorus limitation in our simulations. Sensitivity of the model to fish predation indicates the need for better fish models. A temperature alteration affected all model compartments in the same fashion - general temporal shifts in the curves. However, this is only a very gross picture of temperature effects, and more detailed analyses should be performed.

7. REFERENCES

- Atwater, M. A.; Ball, J. T.; and Brown, P. S. 1973. *The radiation budget of Lake Ontario including cloud coverage*. The Center for the Environment and Man Report No. 4130-97, preliminary results.
- Azad, H. S., and Borchardt, J. A. 1969. A method for predicting the effects of light intensity on algal growth and phosphorus assimilation. *J. Water Poll. Cont. Fed.* 41:R392-418.
- Bloomfield, M. A.; Park, R. A.; Scavia, D.; and Zahorcak, C. S. 1973. Aquatic modeling in the Eastern Deciduous Forest Biome, U.S. International Biological Program. In *Modeling the eutrophication process*, eds. E. J. Middlebrooks, D. H. Falkenberg, and T. E. Maloney, pp. 139-58. Ann Arbor, Michigan: Ann Arbor Science.
- Bogdan, K. G., and McNaught, D. C. 1975. Selective Feeding by Diaptoms and Daphnia. *Verh. Internat. Verein. Limnol.* 19:2935-42.
- Burns, C. W. 1969. Relation between filtering rate, temperature, and body size in four species of Daphnia. *Limnol. and Oceanog.* 14:693-700.
- Burns, N. M., and Pashley, A. E. 1974. In situ measurements of the settling velocity profile of particulate organic carbon in Lake Ontario. *J. Fish. Res. Bd. Canada* 31:291-97.
- Canale, R. P.; DePalma, L. M.; and Vogel, A. H. 1975. *A food web model for Lake Michigan, part 2 - Model formulation and preliminary verification*. Michigan Sea Grant Technical Report 43.
- Canale, R. P., and Vogel, A. H. 1974. Effects of temperature on phytoplankton growth. *J. Environ. Eng. Div., ASCE* 100:231-41.
- Chen, C. W. 1970. Concepts and utilities of ecological models. *J. San. Eng. Div., ASCE* 96:1085-96.
- Chen, C. W. and Orlob, G. T. 1975. Ecological simulation for aquatic environments. In *Systems analysis and simulation in ecology*, vol. 3, ed. B. E. Patton, pp. 475-588. New York: Academic Press.
- Comita, G. W. 1968. Oxygen consumption in Diaptomus. *Limnol. and Oceanog.* 13:51-57.
- Cordeiro, C. F.; Echelberger, W. F.; and Verhoff, F. H. 1973. Rates of carbon, oxygen, nitrogen, and phosphorus cycling through microbial populations in stratified lakes. In *Modeling the eutrophication process*, eds. E. J. Middlebrooks, D. H. Falkenberg, and T. E. Maloney, pp. 111-20. Ann Arbor, Michigan: Ann Arbor Science.
- Department of the Environment (Canada), Atmospheric Environment Service. 1972-73. IFYGL weather data. (Published monthly for April 1972 to June 1973.)

- DiToro, D. M.; O'Connor, D. J.; Thomann, R. V.; and Mancini, J. L. 1975. Phytoplankton-zooplankton - nutrient interaction model for western Lake Erie. In *System analysis and simulation in ecology*, vol. 3, ed. B. C. Patton, pp. 424-75. New York: Academic Press.
- DiToro, D. M.; Thomann, R. V.; and O'Connor, D. J. 1971. A dynamic model of phytoplankton populations in the Sacramento-San Joaquin delta. In *Nonequilibrium systems in natural water chemistry*, vol. 3, ed. B. C. Patton, pp. 424-75, Advances in Chemistry Series, vol. 106. Washington, D.C.: American Chemical Society.
- Dobson, H. F.; Gilbertson, M.; and Sly, P. G. 1974. A summary and comparison of nutrients and related water quality in Lakes Erie, Ontario, Huron, and Superior. *J. Fish. Res. Bd. Canada* 31:731-38.
- Dodson, S. I. 1972. Mortality in a population of *Daphnia rosea*. *Ecol.* 53:1011-23.
- Dugdale, R. C. 1967. Nutrient limitation in the sea: Dynamics, identification and significance. *Limnol. and Oceanog.* 12:685-95.
- Eadie, B. J., and Robertson, A. 1976. An IFYGL carbon budget for Lake Ontario. *J. Great Lakes Res.* (in review).
- Edmondson, W. T. 1957. Trophic relations of the zooplankton. *Trans. of Am. Microsp. Soc.* 76:225-46.
- Eppley, R. W. 1972. Temperature and phytoplankton growth in the sea. *Fish. Bull.* 70:1063-85.
- Eppley, R. W.; Rogers, J. N.; and McCarthy, J. J. 1969. Half-saturation constants for uptake of nitrate and ammonia by marine phytoplankton. *Limnol. and Oceanog.* 14:912-20.
- Fogg, G. E. 1965. *Algal cultures and phytoplankton ecology*. Madison, Wisconsin: University of Wisconsin Press.
- Fuhs, W. G.; Demmerle, S. D.; Canelli, E.; and Chen, M. 1972. Characterization of phosphorus-limited plankton algae (with reflections on the limiting nutrient concept). In *Nutrients and eutrophication*, vol. 1, ed. G. E. Likens, pp. 113-32. Lawrence, Kansas: Allen Press, Inc.
- Glooschenko, W. A.; Moore, J. E.; Munawar, M.; and Vollenweider, R. A. 1974. Primary production in Lakes Ontario and Erie: A comparative study. *J. Fish. Res. Bd. Canada.* 31:253-63.
- Goldman, J. C., and Carpenter, E. J. 1974. A kinetic approach to the effect of temperature on algal growth. *Limnol. and Oceanog.* 19:756-66.
- Goodall, D. W. 1975. Ecosystem modeling in the desert biome. In *Systems analysis and simulation in ecology*, ed. B. C. Patton, pp. 73-94. New York: Academic Press.

- Hall, D. J. 1964. An experimental approach to the dynamics of a natural population of Daphnia galeata mendotae. *Ecol.* 45:94-112.
- Halmann, M., and Stiller, M. 1974. Turnover and uptake of dissolved phosphate in freshwater. A study in Lake Kinneret. *Limnol. and Oceanog.* 19:774-83.
- Hammerling, F. D. 1971. KUTTA. In *The computing technology center numerical analysis library*, eds. G. W. Westly and J. A. Watts. Oak Ridge, Tennessee: Union Carbide Corp.
- Hutchinson, G. E. 1967. *A treatise on limnology, vol. 2: Introduction to lake biology and the limnoplankton*. New York: J. Wiley and Sons.
- Johnson, M. G., and Brinkhurst, R. O. 1971a. Associations and species diversity in benthic macroinvertebrates of Bay of Quinte and Lake Ontario. *J. Fish. Res. Bd. Canada* 28:1683-97.
- Johnson, M. G., and Brinkhurst, R. O. 1971b. Production of benthic macroinvertebrates of Bay of Quinte and Lake Ontario. *J. Fish. Res. Bd. Canada* 28:1699-1714.
- Johnson, M. G., and Brinkhurst, R. O. 1971c. Benthic community metabolism in Bay of Quinte and Lake Ontario. *J. Fish. Res. Bd. Canada* 28:1715-26.
- Jonnassen, P. M. 1972. Ecology and production of the profundal benthos in relation to phytoplankton in Lake Esrom, Copenhagen. *Oikos. Supplementum* 14:1-148.
- Kanwisher, N. 1963. On exchange of gases between the atmosphere and the sea. *Deep Sea Res.* 10:195-207.
- Ketchum, B. H. 1939. The absorption of phosphate and nitrate by illuminated cultures of Nitzschia closterium. *Am. J. Botany* 26:399-407.
- Kibby, H. V. 1971. Energetics and population dynamics of Diaptomus gracilis. *Ecol. Monographs* 41:311-27.
- Larson, D. P.; Mercier, H. T.; and Malueq, K. W. 1973. Modeling algal growth dynamics in Shagawa Lake, Minnesota, with comments concerning projected restoration of the lake. In *Modeling the eutrophication process*, ed. E. J. Middlebrooks, D. N. Fulkenborg, and T. E. Malony, pp. 15-32. Ann Arbor, Michigan: Ann Arbor Science.
- Liss, P. S. 1973. Processes of gas exchange across an air water interface. *Deep Sea Res.* 20:221-38.
- Ludwigson, J. O. 1974. *Two nations, one lake - science in support of Great Lakes management*. Ottawa, Canada: Canadian National Committee for the International Hydrological Decade.

- Lund, J. W. B. 1959. Buoyancy in relation to the ecology of the fresh-water phytoplankton. *Brit. Phycol. Bull.* 1:1.
- MacIssac, J. J., and Dugdale, R. C. 1969. The kinetics of nitrate and ammonia uptake by natural populations of marine phytoplankton. *Deep Sea Res.* 16:45-57.
- McAllister, C. D. 1970. Zooplankton rations, phytoplankton mortality, and estimation of marine production. In *Marine food chains*, ed. J. H. Steele, pp. 419-57. Berkley, California: University of California Press.
- McNaught, D. S., and Scavia, D. 1976. Application of a model of zooplankton composition to problems of fish introductions to the Great Lakes. In *Mathematical modeling of biochemical process in aquatic ecosystems*, ed. R. P. Canale, pp. 281-304. Ann Arbor, Michigan: Ann Arbor Science.
- McNown, J. S., and Malaika, J. 1950. Effects of particle shape on settling velocity at low Reynolds numbers. *Trans. Am. Geophys. Union* 31:74-82.
- McQueen, D. J. 1969. Reduction of zooplankton standing stocks by predaceous Cyclops bicuspidatus thomasi in Marion Lake, British Columbia. *J. Fish. Res. Bd. Canada* 26:1605-18.
- Middlebrooks, E. J.; Falkenborg, D. H.; and Maloney, T. E., eds. 1973. *Modeling the eutrophication process*. Ann Arbor, Michigan: Ann Arbor Science.
- Munawar, M., and Nauwerck, A. 1971. *The composition and horizontal distribution of phytoplankton in Lake Ontario during the year 1970*. Proceedings of the 14th conference on Great Lakes research, pp. 69-78. International Association for Great Lakes Research.
- Munawar, M.; Stadelmann, P.; and Munawar, I. F. 1974. *Phytoplankton biomass, species composition, and primary production at a nearshore and a midlake station of Lake Ontario during IFYGL (IFYGL)*. Proceedings of the 17th conference on Great Lakes research, pp. 629-51. International Association for Great Lakes Research.
- Munk, W. H., and Riley, G. A. 1952. Adsorption of nutrients by aquatic plants. *J. Mar. Res.* 11:215-40.
- Nalepa, T. F. 1972. *An ecological evaluation of a thermal discharge. Part III: The distribution of zooplankton along the western shore of Lake Erie*. Michigan State University, Institute for Water Resources, Technical Report No. 15.
- O'Connor, D. J.; DiToro, D. M.; and Thomann, R. V. 1975. Phytoplankton models and eutrophication problems. In *Ecological modeling in a resource management framework*, ed. C. S. Russel, pp. 149-210. Washington, D.C.: Resources for the Future, Inc.
- O'Neill, R. V. 1969. Indirect estimation of energy fluxes in animal food webs. *J. Theor. Biol.* 22:284-90.

- O'Neill, R. V.; Goldstein, R. A.; Shugart, H. H.; and Mankin, J. B. 1972. *Terrestrial ecosystem energy model*. Eastern Deciduous Forest Biome - International Biological Program Report 72-19.
- Park, P. K. 1969. Oceanic CO₂ system: An evaluation of ten methods of investigation. *Limnol. and Oceanog.* 14:179-86.
- Park, R. A.; O'Neill, R. V.; Bloomfield, J. A.; Shugart, H. H.; Booth, R. S.; Goldstein, R. A.; Mankin, J. B.; Koonce, J. F.; Scavia, D.; Adams, M. S.; Clesceri, L. S.; Colon, E. M.; Dettmann, E. H.; Hoopes, J.; Huff, D. D.; Katz, S.; Kitchell, J. F.; Kohberger, R. C.; LaRow, E. J.; McNaught, D. C.; Peterson, J.; Titus, J.; Weiler, P. R.; Wilkinson, J. W.; and Zahorcak, C. S. 1974. A generalized model for simulating lake ecosystems. *Simulation* 23:33-50.
- Park, R. A.; Scavia, D.; and Clesceri, N. L. 1975. CLEANER, the Lake George model. In *Ecological modeling in a resource management framework*, ed. C. S. Russel, pp. 49-82. Washington, D.C.: Resources for the Future, Inc.
- Parsons, T. R.; LeBresseur, R. J.; Fulton, J. D.; and Kennedy, O. D. 1969. Production studies in the Strait of Georgia II secondary production under the Fraser River plume, February to May, 1967. *J. Exp. Mar. Biol. Ecol.* 3:39-50.
- Pasciak, W. J., and Gavis, J. 1974. Transport limitation of nutrient uptake in phytoplankton. *Limnol. and Oceanog.* 19:881-88.
- Patalas, K. 1969. Composition and horizontal distribution of crustacean plankton in Lake Ontario. *J. Fish Res. Bd. Canada* 26:2135-64.
- Patrick, R., and Reimer, C. W. 1966. *The diatoms of the United States, vol. 1*. Philadelphia, Pennsylvania: Academy of Natural Sciences of Philadelphia.
- Pickett, R., and Eadie, B. J. 1976. Lake Ontario mean surface temperature. In *IFYGL Bulletin* No. 17:59.
- Richards, T. L.; Dragert, H.; and McIntyre, D. R. 1966. Influence of atmospheric stability and over-water pitch on winds over the lower Great Lakes. *Mon. Weather Rev.* 94:448-53.
- Richman, S. 1958. The transformation of energy by Daphnia pulex. *Ecol. Monographs* 28:273-91.
- Richman, S. 1966. The effect of phytoplankton concentration on the feeding rate of Diaptomus oregonensis. *Verh. Internat. Verein. Limnol.* 16:392-98.
- Russel, C. S., ed. 1975. *Ecological modeling in a resource management framework*. Washington, D.C.: Resources for the Future, Inc.

- Ryther, I. H., and Guillard, R. R. L. 1962. Studies of marine planktonic diatoms. Part 3: Some effects of temperature on respiration of five species. *Can. J. Microbiol.* 8:447-53.
- Scavia, D., and Park, R. A. 1976. Documentation of selected constructs and parameter values in the aquatic model, CLEANER. *Ecol. Modeling* 2:33-58.
- Shiomi, M. T., and Chawla, V. K. 1970. *Nutrients in Lake Ontario*. In Proceedings of the 13th conference on Great Lakes research, pp. 715-32. International Association for Great Lakes Research.
- Shugart, H. H.; Goldstein, R. A.; O'Neill, R. V.; and Mankin, J. B. 1974. TEEM: A terrestrial ecosystem energy model for forests. *Oecol. Plant.* 9:231-64.
- Smayda, T. I. 1970. The suspension and sinking of phytoplankton in the sea. *Oceanog. Mar. Biol. Ann. Rev.* 8:353-414.
- Smayda, T. I. 1974. Some experiments on the sinking characteristics of two freshwater diatoms. *Limnol. and Oceanog.* 19:628-35.
- Smayda, T. I., and Boleyn, B. J. 1965. Experimental observations on the floatation of marine diatoms. Part I: Thalassiosira c.f. naria, T. rotula, and Nitzschia seriata. *Limnol. and Oceanog.* 10:499-510.
- Smayda, T. I., and Boleyn, B. J. 1966a. Experimental observations on the floatation of marine diatoms. Part II: Skeletonema custaton and Rhizosolenia setigira. *Limnol. and Oceanog.* 11:18-34.
- Smayda, T. I., and Boleyn, B. J. 1966b. Experimental observations on the floatation of marine diatoms. Part III: Bacteriastrum hyleniun and Chaeteceros lauderi. *Limnol. and Oceanog.* 11:35-43.
- Smith, W. E. 1970. Tolerance of Mysis relicta to thermal shock and light. *Trans. Am. Fish. Soc.* 99:418-22.
- Stadleman, P.; Moore, J. E.; and Pickett, E. 1974. Primary productivity in relation to temperature, structure, biomass concentration, and light conditions at an inshore and offshore station in Lake Ontario. *J. Fish. Res. Bd. Canada* 31:1215-32.
- Steele, J. H. 1974. *The structure of marine ecosystems*. Cambridge, Massachusetts: Harvard University Press.
- Stoermer, E. F.; Bowman, M. W.; Kingston, J. C.; and Schaedel, A. L. 1974. *Phytoplankton composition and abundance in Lake Ontario during IFYGL*. University of Michigan, Great Lakes Research Division, Special Report 53.
- Stumm, W., and Morgan, J. J. 1970. *Aquatic chemistry*. New York: Wiley Interscience.

- Sundaram, T. R., and Rehm, R. G. 1973. The seasonal thermal structure of deep temperate lakes. *Tellus* 25:157-67.
- Suschenya, L. M. 1958. Kolichestvennyĕ dannĕye o fil'tratsionnom pitanii-p-lanktonnykh rachkov. *Nauch. Dokl. Vyssh. Shk., Biol. Nauki.* 1: 241-60. (Original not seen.)
- Suschenya, L. M. 1970. Food rations, metabolism, and growth of crustaceans. In *Marine food chains*, ed. J. H. Steele, pp. 127-41. Berkley, California: University of California Press.
- Sykes, R. M. 1974. Theory of multiple limiting nutrients. *J. Water Poll. Cont. Fed.* 46:2387-92.
- Thomann, R. V.; DiToro, D. M.; Winfield, R. P.; and O'Connor, D. J. 1975. Mathematical modeling of phytoplankton in Lake Ontario. Part I: Model development and verification. Environmental Protection Agency, National Environmental Research Center, EPA-660/3-75-005.
- Watson, N. H. F., and Carpenter, G. F. 1974. Seasonal abundance of crustacean zooplankton and net plankton biomass of Lakes Huron, Erie, and Ontario. *J. Fish. Res. Bd. Canada* 31:309-17.
- Wolvekamp, H. P., and Waterman, T. H. 1960. Respiration. In *The physiology of crustacea. Volume 1: Metabolism and growth*, ed. T. H. Waterman, pp. 35-100. New York: Academic Press.
- Weast, R. C., ed. 1973. *Handbook of chemistry and physics*. Cleveland, Ohio: CRC Press.
- Zahorcak, C. S. 1974. Formulation of a numbers-biomass model for simulating the dynamics of aquatic insect populations. Eastern Deciduous Forest Biome. *International Biological Program Report* 74-75.
- Zeuthen, E. 1947. Body size and metabolic rate in the animal kingdom. *Comp. Rend. Lab. Carlsberg, Ser. Chim.* 26:17-161.
- Zeuthen, E. 1953. Oxygen uptake as related to body size in organisms. *Quart. Rev. Biol.* 28:1-12.

APPENDIX A. MODEL COEFFICIENTS AND INITIAL CONDITIONS

The coefficient values and initial conditions used in the calibration of our model are in tables A.1, A.2, and A.3. The equations describing the dynamics of the biological and chemical processes in the model are in Appendix B.

A.1 Phytoplankton Coefficients

The maximum respiration rate, B_1 , is assumed to be 0.09/day. This is consistent with the data compiled by DiToro et al. (1971), i.e., approximately 0.05-0.1/day. G_{MAX} , the maximum growth rate, is set equal to 1.8/day, a value within the range of most measurements (Goldman and Carpenter, 1974).

The non-predatory mortality rate is considered relatively unimportant under conditions of healthy growth and sublethal temperatures. We consider that during stressful periods but at sublethal temperatures, the death rate (B_2) will increase a maximum of 3 percent per day.

For lack of detailed information concerning the relative effect of temperature on different groups of phytoplankton, we assume that temperature effects on photosynthesis and respiration for all groups are the same. Therefore the values for $TOPT$, $TMAX$, and Q_{10} are the same. A value of 2.1 is used for Q_{10} . Goldman and Carpenter (1974) report a value of 2.19 for two species; Eppley (1972) reports 1.8. Canale and Vogel (1974) compiled data relating growth rate to temperature. Q_{10} values estimated from their data ranged from about 2.0-3.0. The optimum temperature, $TOPT$, is 20 °C (Patrick and Reimer, 1966; Ryther and Guillard, 1962; Fogg, 1965). $TMAX$, the maximum temperature, is taken as 35°C (Patrick and Reimer, 1966; Canale and Vogel, 1974).

The limitation of photosynthesis is dependent on three coefficients: the saturating light intensity (XIS) and the half-saturation constants for phosphorus (XKP) and nitrogen (XKN). A value of 300 langlys/day is commonly used for XIS (DiToro et al., 1971; Canale et al., 1975). The half-saturation constant for phosphorus has generally been reported between 0.001 and 0.01 mg-P/l (Halmann and Stiller, 1974; Fuhs et al., 1972; DiToro et al., 1971). We obtain best results by using 0.009 mg-P/l. The half-saturation constant for nitrogen is based on total available nitrogen ($NH_3 + NO_3$). Eppley et al. (1969) measured constants for many cultures growing on nitrate and ammonia separately and found an average value of 0.026 mg-N/l and 0.028 mg-N/l, respectively. DiToro et al. (1971) compiled constants from the literature and found an average of 0.029 with a range of 0.0014-0.130 mg-N/l. We use a value of 0.027 mg-N/l and assume a preference factor of 2.0 (i.e., for equal concentrations of NH_3 and NO_3 , twice as much NH_3 will be absorbed).

Other phytoplankton-related coefficients are the extinction coefficient of Lake Ontario water and the coefficient relating phytoplankton carbon to the overall extinction coefficient (table A.1). The extinction coefficient of Lake Ontario water is taken as 0.2/m (Thomann et al., 1975), and the phytoplankton coefficient as 0.3/m/mg-C/l (Azad and Borchardt, 1969).

Table A.1. Phytoplankton Coefficients

Symbol	Description	Value
XNC	N:C ratio in biomass (weight)	0.18
PC	P:C ratio in biomass (weight)	0.024
EPS	Extinction coefficient of Lake Ontario water (m^{-1})	0.2
B	Phytoplankton extinction coefficient ($mg-c/l$)	0.3
α	Preference factor	2

A.2 Remineralization Constants

The first order decay rates for detritus, organic nitrogen, and ammonia are 0.001, 0.001, and 0.003/(day °C), respectively. These values are consistent with most modeling efforts (DiToro et al., 1975; O'Connor et al., 1975; Canale et al., 1975; Chen, 1970).

The weight ratio of nitrogen to carbon (XNC) is 0.18 and P:C (PC) is 0.024, assuming an atomic stoichiometry of $C_{106}N_{16}P_1$ (Cordeiro et al., 1973).

A.3 Zooplankton Coefficients

In order to obtain estimates for the zooplankton coefficient values, we selected a representative form for each group modeled. The following genera are considered typical for the crustacean groups of interest in Lake Ontario:

- Large cladocerans - Daphnia
- Small cladocerans - Bosmina
- Herbivorous copepods - Diaptomus
- Carnivorous zooplankton - Cyclops
- Mysids - Mysis.

General characteristics of the rotifers were obtained from Hutchinson (1967).

Preferential feeding by zooplankton is characterized by the food coefficients in table A.2. Based on the work of Bogdan and McNaught (1975), we assume that there is relatively little food preference by large cladocerans over the range of particle sizes in the model. Thus, we set all the preference coefficients equal to 1.0 for this group. For lack of any information on feeding preference of small cladocerans, such a course is also adopted for them. *Diaptomus* has been found to prefer small particles over large ones by a ratio of 4:1 (Bogdan and McNaught, 1975); thus the coefficients for herbivorous copepods are set at 1.0 and 0.25 for the two particle sizes, respectively.

Table A.2. Assimilation and Preference Coefficients. Upper Number is ASM and Lower Number is PREF. (Index 16 refers to mysids.)

	(i)	(j)					
		5	6	7	8	15	16
Small Diatoms	1	0.5 1	0.5 1	0.5 1	0.5 0.8		0.5 1
Large Diatoms	2	0.5 1	0.5 1	0.5 0.25	0.5 0.2		0.5 1
Small Others	3	0.5 1	0.5 1	0.5 1	0.5 1		0.5 1
Large Others	4	0.5 1	0.5 1	0.5 0.25	0.5 0.2		0.5 1
Small Cladocerans	5					0.5 0.5	
Large Cladocerans	6					0.5 0.5	
Herbivores	7					0.5 0.5	
Rotifers	8					0.5 1	
Detritus	14	0.2 1	0.2 1	0.2 1	0.2 1		0.5 1
Carnivores	15					0.5 0.2	

Hutchinson (1967) reviewed many works related to rotifer feeding. His summary shows that rotifers generally grow better on smaller particles (<20 μ in maximal diameter). Some of the reports also indicate a preference for green algae over diatoms. Thus, the preference factors for large diatoms, large non-diatoms, small diatoms, small non-diatoms, and detritus have been set at 0.2, 0.2, 0.8, 1.0, and 1.0, respectively.

The carnivorous zooplankton (especially cyclopoids) feed mainly on small zooplankters, including rotifers, calanoid nauplii, early life stages of cladocerans, and their own young (Hutchinson, 1967; McQueen, 1969). Since we do not have information on the food preference for the potential prey, but assume adult crustaceans are large enough to be difficult to catch, we set the preferences for large and small cladocerans and herbivorous copepods at 0.5. We assume rotifers, being smaller, are preyed upon at all times (preference = 1.0). Cannibalism is set at a constant fraction of the available carnivorous zooplankton population (preference = 0.2).

The final link in the food web is fish predation. The coefficients are somewhat arbitrary at this time since we do not dynamically model fish populations. Small cladocerans are assumed to escape some predation and therefore have a lower loss rate (PCT = 0.04) than large cladocerans and herbivorous copepods (PCT = 0.05). The loss of carnivorous zooplankton to fish predation is assumed as 1 percent per day, while mysids, a desirable fish prey, are lost at 10 percent per day.

All zooplankton assimilation is assumed 50 percent efficient on phytoplankton and zooplankton foods and 20 percent efficient on detrital foods (Suschenya, 1970; Kibby, 1971; Edmondson, 1957).

Physiological death is assumed to be low at sublethal temperatures. Hall (1964) reported non-predatory mortality to be less than 4 percent per day for Daphnia galeata mendotae. Dodson (1972) found that only 6.5 percent of the mortality could be attributed to non-predatory losses for a population of Daphnia rosea. We use an exponential loss rate of 1 percent per day for all zooplankton groups.

The half-saturation constant for feeding (XKG) is calculated from Richmann (1966) for Diaptomus oregonensis (13×10^3 cells/ml at 20° C). We convert this to 0.16 mg-C/l by assuming 1.2×10^{-8} mg-C/cell (based on Chlorella, 6 μ diameter, 1 g/cc density, 0.1 g-C/g wet wt., sphere). For lack of other data, this value is used for all the herbivore groups.

The food of carnivorous zooplankton is generally less abundant than that of herbivorous forms, and the carnivores have most likely adapted by evolving a lower half-saturation constant. Specifically, we assume an XKG for carnivores approximately an order of magnitude less than that for herbivores (XKG = 0.02). This approximation is based on the observation that the carnivores' food (herbivores) are roughly an order of magnitude less abundant than the herbivores' food.

McAllister (1970) found that feeding stopped below 0.016 mg-C/l for a marine copepod. Steele (1974) shows results of experiments by Parsons

et al. (1969) where this minimum level seems to vary between 5×10^5 and $20 \times 10^3 \mu^3/\text{ml}$ (0.05 - 0.2 mg-C/l). We use a value of 0.05 mg-C/l for XMIN for all herbivorous zooplankters. The minimum level of zooplankton necessary to stimulate higher trophic level predation (XMIN = 0.0025) is based on the measured winter population densities.

Both grazing and respiration rates are assumed to be dependent on temperature with a Q10 of 2.4. The Q10's for respiration in crustaceans usually range between 2 and 3 (Wolvekamp and Waterman, 1960). Specifically, a Q10 of 2.2 has been obtained for Diaptomus oregonensis, an important herbivore in Lake Ontario (Comita, 1968); and unpublished studies by one of the authors (Robertson) have shown a value a little below 3 for Mysis relicta, another important Lake Ontario form. The available information seems inadequate to permit the selection of different values for the various types of zooplankton in our model, and so 2.4 is chosen as a representative, intermediate value and applied to all zooplankton types.

For grazing rate, there is even less information available on the Q10's of Great Lakes forms. It is assumed that metabolic and related feeding rates are related to temperature in much the same way as respiration. Thus, the same Q10 has been chosen. In support of this, Burns (1969) finds a Q10 of 2.71 for the feeding rate of Daphnia galeata, a Lake Ontario herbivore.

As there is little information available on temperature tolerances, the optimum and maximum temperatures for respiration and feeding are selected from general considerations of the geographical and seasonal distributions of the various forms. Small cladocerans and rotifers are considered the most tolerant of elevated temperatures; and the maximum temperature for feeding for both of them is set at 30° C, which is roughly the warmest temperature they normally face in the Great Lakes. It is commonly observed that the optimum temperature is quite close to the maximum, and so the optimum is set two degrees lower (28° C) for these two forms. Respiration is assumed to be slightly more tolerant of high temperatures, and the optimum and maximum are set at 30° and 32° C, respectively, for this process.

The logic for setting the thermal limits for the other forms (table A.3) is similar to that for the small cladocerans and rotifers. However, consideration of the relative occurrences of the various types led to lowering the optima and maxima for large cladocerans and carnivorous zooplankton several degrees and for herbivorous copepods a further 4° or so. The much lower limits for mysids are based on the results of thermal tolerance studies on Mysis relicta conducted by Smith (1970).

Maximum grazing rates at optimum temperature (A1) are estimated largely from filtering rate measurements in the literature. The literature values at given temperatures are converted to maximum grazing rates at optimum temperature by multiplying by the lowest algal concentration for maximum food intake and then correcting to optimum temperature assuming a Q10 of 2.4 over the interval between measured and optimum.

Table A.3. Model Coefficients

Symbol	Description	Units	1	2	3	4	5	6	7	8
A1	Maximum consumption rate at optimum temperature	g/g/day	--	--	--	--	1.9	1.7	1.7	2.2
B1	Maximum respiration rate at optimum temperature	g/g/day	0.09	0.09	0.09	0.09	0.36	0.26	0.31	0.40
B2	Maximum mortality rate below critical temperature	g/g/day	0.03	0.03	0.03	0.03	0.01	0.01	0.01	0.01
	First order decay rate at 1°C	g/g/day	--	--	--	--	--	--	--	--
GPMAX	Maximum growth rate at optimum temperature	g/g/day	1.8	1.8	1.8	1.8	--	--	--	--
PCT	Loss rate due to higher level predation	g/g/day	--	--	--	--	0.04	0.05	0.05	--
Q ₁₀	Slope of suboptimal temperature curve	GROWTH RESPIRATION	-- --	2.1 2.1	2.1 2.1	2.1 2.1	2.1 2.4	2.4 2.4	2.4 2.4	2.4 2.4
TOPT	Optimum temperature for process	GROWTH RESPIRATION	°C °C	20 20	20 20	20 20	20 30	28 28	26 24	28 30
TMAX	Maximum temperature for process	GROWTH RESPIRATION	°C °C	35 35	35 35	35 35	35 32	30 30	28 26	30 32
XIS	Saturating light intensity for photosynthetic growth	langley's day	300	300	300	300	--	--	--	--
XKG	1/2-saturation constant for grazing	mg-c/l	--	--	--	--	0.16	0.16	0.16	0.16
XKP	1/2-saturation constant for growth on P	mg-P/l	0.009	0.009	0.009	0.009	--	--	--	--
XKN	1/2-saturation constant for growth on N	mg-N/l	0.027	0.027	0.027	0.027	--	--	--	--
XMIN*	Minimum food level necessary to stimulate consumption	mg-c/l	--	--	--	--	0.05	0.05	0.05	0.05
XMASSI	Initial conditions (assume equal in all 3 segments)	mg/l	0.025	0.025	0.025	0.025	0.002	0.002	0.002	0.002

The filtering rate of 2.5 ml/animal/day obtained by Richman (1966) for Diaptomus oregonensis at approximately 20° C is taken as representative of the herbivorous copepods. This is converted to units of liters/milligrams zooplankton-C/day by assuming that the average dry weight per individual copepod was 8.0 µg (Nalepa, 1972) and that 50 percent of the dry weight is carbon. Similar procedures are followed for large cladocerans based on Richman's (1958) value for Daphnia pulex (4.5 ml/day at 20° C), and for small cladocerans based on the middle of the range presented by Hutchinson (1967) from work by Suschenya (1958) for Bosmina longirostris (2.0 ml/day at an assumed 20° C).

Richman (1966) has studied the relation between food concentration and food intake of Diaptomus oregonensis. He determines a value of approximately

Table A.3. Model Coefficients (continued)

Symbol	Description	Units	9	10	11	12	13	14	15	16
A1	Maximum consumption rate at optimum temperature	g/g/day	--	--	--	--	--	--	1.6	1.0
B1	Maximum respiration rate at optimum temperature	g/g/day	--	--	--	--	--	--	0.30	0.21
B2	Maximum mortality rate below critical temperature	g/g/day	--	--	--	--	--	--	0.01	0.01
	First order decay rate at 1°C	g/g/day	--	0.001	0.003	--	--	0.001	--	--
GPMAX	Maximum growth rate at optimum temperature	g/g/day	--	--	--	--	--	--	--	--
PCT	Loss rate due to higher level predation	g/g/day	--	--	--	--	--	--	0.01	0.1
Q ₁₀	Slope of suboptimal temperature curve	GROWTH RESPIRATION	-- --	-- --	-- --	-- --	-- --	-- --	2.4 2.4	2.4 2.4
TOPT	Optimum temperature for process	GROWTH RESPIRATION	°C °C	-- --	-- --	-- --	-- --	-- --	26 27	15 16
TMAX	Maximum temperature for process	GROWTH RESPIRATION	°C °C	-- --	-- --	-- --	-- --	-- --	27 28	16 17
XIS	Saturating light intensity for photosynthetic growth	langleys day	--	--	--	--	--	--	--	--
XXG	1/2-saturation constant for grazing	mg-c/l	--	--	--	--	--	--	0.02	0.10
XKP	1/2-saturation constant for growth on P	mg-P/l	--	--	--	--	--	--	--	--
XKN	1/2-saturation constant for growth on N	mg-N/l	--	--	--	--	--	--	--	--
XMIN*	Minimum food level necessary to stimulate consumption	mg-c/l	--	--	--	--	--	--	0.01	0.05
XMASSI	Initial conditions (assume equal in all 3 segments)	mg/l	0.014	0.1	0.02	0.24	23	0.05	0.002	0.002**

25,000 cells/ml as the lowest concentration with maximum food intake using both Chlamydomonas and Chlorella. Based on earlier work of his (Richman,¹³ 1958), this can be converted to a weight value of approximately 3.1×10^6 mg-C/ml. As similar measurements have not been made for other zooplankters, this value is assumed to apply to the other types of herbivores, i.e., small and large cladocerans.

For carnivorous zooplankton, McQueen's (1969) results for Cyclops bicuspidatus are used to estimate a rate of search (equivalent to a filtering rate of 5 ml/copepod/day). Assuming a dry weight per individual of 5 µg and a composition of 50 percent carbon, this converts to 2.0 l/mg zooplankton C/day (temperature 17.5° C). McQueen's data is also used to obtain a rough

estimate of maximum food intake for carnivorous zooplankton of 0.15 mg prey C/mg predator C/day.

For mysids no information has been found concerning feeding rate. It is assumed that metabolic rates, including feeding rates, decrease somewhat with increasing body size (Zeuthen, 1947 and 1953) and, as mysids are substantially larger than the other zooplankters, their maximum feeding rate should be set lower than that for the other forms. Similar assumptions are made to obtain a feeding rate for the rotifers; however, this group, being much smaller than the other zooplankters, would have a higher rate. Values of 1.0 mg food C/mg mysid C/day and 2.2 mg food C/mg rotifer C/day are used as the maximum rates at optimum temperatures.

The final parameters needed for zooplankton are the respiration rates at optimum temperature. In the same manner as used for feeding rates, the respiration rates at some temperatures are obtained from the literature, converted as necessary to a weight specific rate, and then adjusted to the rate at optimum temperature, assuming a Q10 of 2.4. The rate for herbivorous copepods is based on Comita's (1968) study on Diaptomus oregonensis and for large cladocerans on Richman's (1958) values for Diaphnia pulex. As no appropriate rates were found in the literature for Bosmina or other small cladocerans, the value for this group is obtained from information published by Richman (1958). He presents a graph of dry weight versus oxygen consumption. An average dry weight of 4 μ g is assumed for the small cladocerans and applied to Richman's graph to obtain a respiration rate. For lack of appropriate experimental results, carnivorous zooplankters (mainly cyclopoid copepods) are assumed to have the same maximum respiration rate as the herbivorous copepods. The respiration rates for mysids are based on unpublished results from studies relating respiration to temperature for Mysis relicta conducted by one of the authors (Robertson). Based on the rotifers' relatively smaller body size, their respiration rate at optimum temperature is set at 0.4 mg C/mg C/day, a value somewhat higher than that used for the other zooplankters.

A.4 Initial Conditions

Running a differential equation model for a lake system without external loads, as we do at this stage, it is impossible to establish a steady state solution since there is continual loss to the sediments. With this limitation, the system cannot be run for multiple years to determine its own initial conditions as suggested by Park, Scavia, and Clesceri (1975). Even if loads were included, to use their method, one would have to assume the lake was in equilibrium with the loads. To avoid misleading and transient responses of the equations, an attempt is made to compromise best available initial condition estimates with estimates producing a semi-steady state for a 1-year simulation. In most cases where reliable values are available, the initial conditions used (table A.3) are not far from the literature estimates.

Values for ammonia and nitrate compartments are abstracted from Shiomi and Chawla (1970) and the available phosphorus initial condition is

determined from Dobson et al. (1974). Total phytoplankton carbon of 0.1 mg/l is used as an initial condition and is divided equally among the four groups. This value is determined from the volume estimates of Munawar and Nauwerck (1971) and assumes 1 g wet weight/cm³ and 0.1 g-C/g wet weight. An estimate of the initial crustacean carbon is calculated from Watson and Carpenter (1974). They found 9.9×10^{-3} mg dry weight/l in a 50-m vertical haul. By using a dry weight:carbon ratio of 2.0, we calculate a total crustacean carbon initial condition of 0.005 mg/l. Assuming this value is a low estimate due to the inefficiency of net collection, we use a value of 0.002 mg-C/l for each of the five zooplankton types in the upper waters. This results in a total zooplankton (herbivorous and carnivorous crustaceans plus rotifers) concentration of 0.01 mg-C/l. Initial total inorganic carbon is calculated from pH and alkalinity measurements. Organic nitrogen concentration is our best guess based on data compiled by Thomann et al. (1975), and initial detrital carbon is based on our simulation results.

APPENDIX B. MODEL EQUATIONS

The differential equations describing the dynamics of the biological and chemical variables in the model are given below. The cross-reference matrix (table B.1) indicates the transfer between state variables as equation numbers.

Table B.1. Biological System

Organism or Nutrient (Code Number)	(1)	(2)	(3)	(4)	(5)	(6)	(7)	(8)	(9)
Small Diatoms (1)					2.1	2.1	2.1	2.1	3.1
Large Diatoms (2)					2.1	2.1	2.1	2.1	3.1
Small Others (3)					2.1	2.1	2.1	2.1	3.1
Large Others (4)					2.1	2.1	2.1	2.1	3.1
Small Cladocerans (5)									3.1
Large Cladocerans (6)									3.1
Herbivores (7)									3.1
Rotifers (8)									3.1
Phosphorus (9)	3.2	3.2	3.2	3.2					
Organic Nitrogen (10)									
NH ₃ (11)	5.3	5.3	5.3	5.3					
NO ₃ (12)	6.2	6.2	6.2	6.2					
Carbon (13)	7.2	7.2	7.2	7.2					
Detritus (14)					8.2	8.2	8.2	8.2	3.3
Carnivores (15)									3.1
Mysids (16)									3.1
Benthos (17)									3.1

Table B.1. Biological System (continued)

Organism or Nutrient (Code Number)	(10)	(11)	(12)	(13)	(14)	(15)	(16)	(17)	Other
Small Diatoms (1)	4.1			7.1	8.4		2.1	SED	Sink
Large Diatoms (2)	4.1			7.1	8.4		2.1	SED	Sink
Small Others (3)	4.1			7.1	8.4		2.1	SED	Sink
Large Others (4)	4.1			7.1	8.4		2.1	SED	Sink
Small Cladocerans (5)	4.1			7.1	$\begin{bmatrix} 8.4 \\ 8.1 \end{bmatrix}$	2.3			2.5
Large Cladocerans (6)	4.1			7.1	$\begin{bmatrix} 8.4 \\ 8.1 \end{bmatrix}$	2.3			2.5
Herbivores (7)	4.1			7.1	$\begin{bmatrix} 8.4 \\ 8.1 \end{bmatrix}$	2.3			2.5
Rotifers (8)	4.1			7.1	$\begin{bmatrix} 8.4 \\ 8.1 \end{bmatrix}$	2.3			2.5
Phosphorus (9)									
Organic Nitrogen (10)		4.3							
NH ₃ (11)			5.2						
NO ₃ (12)									
Carbon (13)									
Detritus (14)	4.2			8.3			8.2	SED	Sink
Carnivores (15)	4.1			7.1	$\begin{bmatrix} 8.4 \\ 8.1 \end{bmatrix}$	2.3			2.5
Mysids (16)	4.1			7.1	$\begin{bmatrix} 8.4 \\ 8.1 \end{bmatrix}$				2.5
Benthos (17)									Pred.

PHYTOPLANKTON ($i = 1-4$)

$$\frac{dB_i}{dt} = \text{PHY}_i - \text{RESP}_i - \text{GRAZ}_i - \text{MORT}_i \quad (\text{B.1})$$

$$PHY_i = GP_{MAX_i} * MIN(U_P, U_N, U_I) * TEMP * B_i, \quad (B.1.1)$$

where

GP_{MAX} = maximum growth rate

$$U_P = \frac{PO_4}{PO_4 + XKP_i}$$

XKP = half-saturation constant for P_i

$$U_N = \frac{NO_3 + NH_3}{NO_3 + NH_3 + XKN_i}$$

XKN_i = half-saturation constant for N

$$U_I = \frac{2.718 * FP}{\epsilon' * (Z_2 - Z_1)} \left[e^{-\frac{I_0}{I_s} e^{-\epsilon' Z_2}} - e^{-\frac{I_0}{I_s} e^{-\epsilon' Z_1}} \right]$$

FP = photoperiod

ϵ' = corrected extinction coefficient = $\epsilon + \alpha \epsilon B_i$

ϵ = extinction coefficient of water

Z_2, Z_1 = depth

I_0 = incident solar radiation

I_s = saturating light intensity

$$TEMP = V^X e^{X(1 - V)} \quad (B.1.1.1)$$

$$V = \frac{TMAX_i - T}{TMAX_i - TOPT_i}$$

$$X = \left[\frac{W(1 + \sqrt{1 + 40/W})}{20} \right]^2$$

$$W = \ln(Q_{10}) (TMAX_i - TOPT_i)$$

$TMAX$ = upper lethal temperature

T = temperature

$TOPT$ = optimum temperature

Q_{10} = slope of sub-optimal curve

$$MORT = B2_i [e^{T - TMAX} - (1 - TEMP(1 - U))] * B_i, \quad (B.1.2)$$

where

$$U = \text{MIN}(U_N, U_P, U_I) \text{ (equation B.1.1)}$$

$B2_i$ = maximum natural mortality rate below TMAX

$$\text{RESP}_i = B1_i * \text{TEMP} * B_i, \quad (\text{B.1.3})$$

where

$B1_i$ = maximum respiration rate

$$\text{GRAZ}_i = \sum_j C_{ij} \text{ summed over all predators (equation B.2.1)} \quad (\text{B.1.4})$$

ZOOPLANKTON ($j = 5-8, 15, 16$)

$$\frac{dB_j}{dt} = \text{CON}_j - \text{RESP}_j - \text{MORT}_j - \text{GRAZ}_j - \text{PRED}_j, \quad (\text{B.2})$$

where

$\text{CON}_j = \sum_i C_{ij}$ (summed over all prey)

$$C_{ij} = A1_j * \text{TEMP} * \left[\frac{\text{PREF}_{ij} * B_i - \text{XPMIN}_j}{\sum_i (\text{PREF}_{ij} * B_i) - \sum_i \text{XPMIN}_i + \text{XKGP}_j} \right] * B_j \quad (\text{B.2.1})$$

$$\text{XPMIN}_i = \left[\frac{\text{PREF}_{ij} * B_i}{\sum_i \text{PREF}_{ij} * B_i} \right] \text{XMIN}_j$$

$$\text{XKGP}_j = \left[\frac{\sum_i \text{PREF}_{ij} * B_i - \text{XMIN}_j}{\sum_i \text{PREF}_{ij} * B_i} \right] \text{XKG}_j$$

$A1_j$ = maximum consumption rate

PREF_{ij} = preference factor for i by j

XMIN_j = minimum food level

XKG_j = half-saturation constant for feeding.

$$\text{RESP}_j = B1_j * \text{TEMP} * B_j, \quad (\text{B.2.2})$$

where

$B1_j$ = maximum respiration rate

$$\text{GRAZ}_i = \sum_k C_{jk} \quad (\text{summed over predators}) \quad (\text{B.2.3})$$

$$\text{MORT}_j = B2_j * (1 + e^{T-TMAX}) * B_j, \quad (\text{B.2.4})$$

where $B2_j$ = natural mortality rate below TMAX

$$\text{PRED}_j = \text{PCT}_j * (B_j - XMIN), \quad (\text{B.2.5})$$

where PCT_j = fish predation rate

PHOSPHORUS

$$\frac{dp}{dt} = PC[\text{RTOT} - \text{PTOT} + \text{REMINC}] \quad (\text{B.3})$$

$$\text{RTOT} = \sum \text{RESP} \quad (\text{equations B.1.3 and B.2.2}) \quad (\text{B.3.1})$$

$$\text{PTOT} = \sum \text{PHY} \quad (\text{equation B.1.1}) \quad (\text{B.3.2})$$

$$\text{REMINC} = \text{remineralization} \quad (\text{equation 3.8.3}) \quad (\text{B.3.3})$$

where PC = phosphorus:carbon ratio

ORGANIC NITROGEN

$$\frac{dN}{dt} = \text{XNC}[\text{RTOT} + \text{REMINC}] - \text{REMINO} \quad (\text{B.4})$$

$$\text{RTOT} = \sum \text{RESP} \quad (\text{equations B.1.3 and B.2.2}) \quad (\text{B.4.1})$$

$$\text{REMINC} = \text{remineralization} \quad (\text{equation B.8.3}) \quad (\text{B.4.2})$$

$$\text{REMINO} = B2_N * T * N, \quad (\text{B.4.3})$$

where $B2_N$ = ammonification rate at 1° C
 XNC = nitrogen:carbon ratio

AMMONIA

$$\frac{dNH_3}{dt} = \text{REMINO} - \text{REMINH} - \text{UPTAKE} \quad (\text{B.5})$$

$$\text{REMINO} = \text{ammonification (equation B.4.3)} \quad (\text{B.5.1})$$

$$\text{REMINH} = B_{2_{NH}} * T * NH_3, \quad (\text{B.5.2})$$

where $B_{2_{NH}}$ = nitrification rate at 1° C

$$\text{UPTAKE} = \text{XNC} * \Sigma \text{PHY} * \text{PRF}, \quad (\text{B.5.3})$$

where XNC = nitrogen:carbon ratio

PHY = primary production

$$\text{PRF} = \frac{\alpha_{NH_3}}{\alpha_{NH_3} + \alpha_{NO_3}}$$

α = preference coefficient

NITRATE

$$\frac{dNO_3}{dt} = \text{REMINH} - \text{UPTAKE} \quad (\text{B.6})$$

$$\text{REMINH} = \text{nitrification (equation B.5.2)} \quad (\text{B.6.1})$$

$$\text{UPTAKE} = \text{XNC} * \Sigma \text{PHY} * (1 - \text{PRF}), \quad (\text{B.6.2})$$

where XNC = nitrogen:carbon ratio

PHY = primary production (equation B.1.1)

PRF = preferential uptake term (equation B.5.3)

INORGANIC CARBON

$$\frac{dC}{dt} = \text{RTOT} - \text{PTOT} + \text{REMINC}, \quad (\text{B.7})$$

$$RTOT + ERESP \text{ (equation B.1.3 and B.2.2)} \quad (B.7.1)$$

$$PTOT = \Sigma PHY \text{ (equation B.1.1)} \quad (B.7.2)$$

$$REMINC = \text{remineralization (equation B.8.3)} \quad (B.7.3)$$

DETRITUS

$$\frac{dDET}{dt} = DEF - GRAZ_i - REMINC + MORTOT \quad (B.8)$$

$$DEF = \sum_{ij} C_{ij} (1 - ASM_{ij}) \quad (B.8.1)$$

where C_{ij} = consumption (equation B.2.1)
 ASM_{ij} = assimilation efficiency

$$GRAZ_i = \sum_{ij} C_{ij} \text{ summed over grazers} \quad (B.8.2)$$

$$REMINC = B2_D * T * DET, \quad (B.8.3)$$

where $B2_D$ = decay rate at 1° C

$$MORTOT = \Sigma MORT \text{ (equation B.1.2 and B.2.4)} \quad (B.8.4)$$

APPENDIX C. COMPUTER PROGRAM

The computer program, written in FORTRAN IV and implemented on a CDC 6600 system, consists of 1 main routine, 10 subroutines, 9 functions, and 2 direct access files. Simulation of 1 year at a daily step size plus input and plotting output uses 150 seconds of CPU time and requires approximately 57.5k words of core.

The general solution to the model equations involves evaluation of biological effects, carbon equilibrium, diffusion, and sedimentation:

$$C_{i,n} = \left[C_{i,n-1} + \int_1^2 S_c dt \right] + \left[\frac{\Delta t}{Z_1} (D_{n-1} + A_n + S_n) \right] \quad (\text{see Section 2.1}).$$

The numerical procedure used to evaluate the solutions to the equations consists of two steps: 1) the state variable concentrations described by the coupled differential equations in Appendix B are evaluated by a modified Runge-Kutta-Merson (Hammerling, 1971) algorithm and 2) added to this solution, the diffusion, sedimentation, air/water exchange, and any other "non-instantaneous" transfers, as well as re-establishment of the carbon equilibrium system, at the end of each time step (fig. C.1). The time-separation of these steps is acceptable if the step size is small enough. All simulations are run with a 1-day step size and the diffusion mechanism is calculated from the previous day's data to add additional stability.

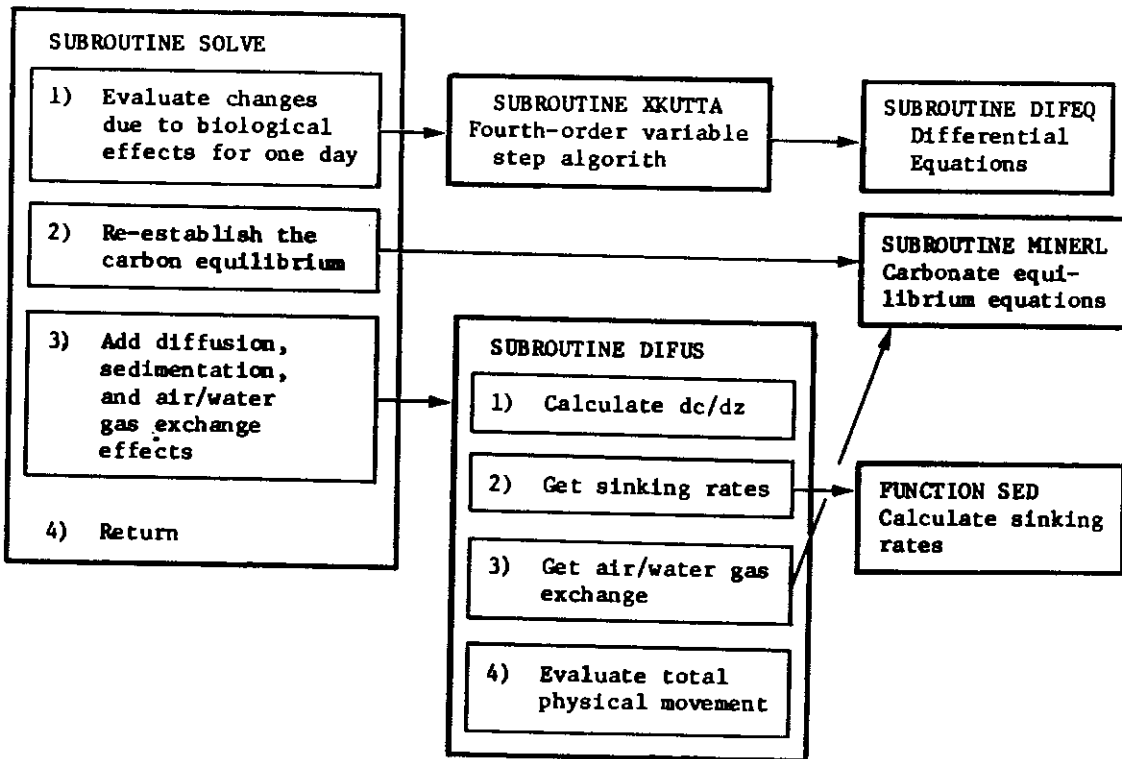


Figure C.1. Model program logic flow.

Environmental Research LABORATORIES

The mission of the Environmental Research Laboratories is to study the oceans, inland waters, the lower and upper atmosphere, the space environment, and the Earth, in search of the understanding needed to provide more useful services in improving man's prospects for survival as influenced by the physical environment. The following laboratories contribute to this mission.

- MESA** *Marine EcoSystems Analysis Program Office.* Plans and coordinates regional programs of basic and applied research directed toward the solution of environmental problems which involve the functioning, health and restoration of marine ecosystems.
- OCSEA** *Outer Continental Shelf Environmental Assessment Program Office.* Plans and directs assessments of the primary environmental impact of energy development along broad areas of the outer continental shelf of the United States; coordinates related research activities of federal, state and private institutions.
- W/M** *Weather Modification Program Office.* Plans and directs ERL weather modification research for precipitation enhancement and severe storms mitigation; operates ERL's research aircraft.
- NHEML** *National Hurricane and Experimental Meteorology Laboratory.* Develops techniques for more effective understanding and forecasting of tropical weather. Research areas include: hurricanes and tropical cumulus systems; experimental methods for their beneficial modification.
- RFC** *Research Facilities Center.* Provides aircraft and related instrumentation for environmental research programs. Maintains liaison with user and provides required operations or measurement tools, logged data, and related information for airborne or selected surface research programs.
- (CIRES)** *Theoretical Studies Group.* Provides NOAA participation in the Cooperative Institute for Research in Environmental Sciences (CIRES), a joint activity with the University of Colorado. Conducts cooperative research studies of a theoretical nature on environmental problems.
- AOML** *Atlantic Oceanographic and Meteorological Laboratories.* Research areas include: geology and geophysics of ocean basins and borders, oceanic processes, sea-air interactions and remote sensing of ocean processes and characteristics (Miami, Florida).
- PMEL** *Pacific Marine Environmental Laboratory.* Research areas include: environmental processes with emphasis on monitoring and predicting the effects of man's activities on estuarine, coastal, and near-shore marine processes (Seattle, Washington).
- GLERL** *Great Lakes Environmental Research Laboratory.* Research areas include: physical, chemical, and biological limnology; lake-air interactions, lake hydrology, lake level forecasting, and lake ice studies (Ann Arbor, Michigan).
- GFDL** *Geophysical Fluid Dynamics Laboratory.* Research areas include: dynamics and physics of geophysical fluid systems; development of a theoretical basis, through mathematical modeling and computer simulation, for the behavior and properties of the atmosphere and the oceans (Princeton, New Jersey).
- APCL** *Atmospheric Physics and Chemistry Laboratory.* Research areas include: processes of cloud and precipitation physics; chemical composition and nucleating substances in the lower atmosphere; laboratory and field experiments toward developing feasible methods of weather modification.
- NSSL** *National Severe Storms Laboratory.* Research is directed toward improved methods of predicting and detecting tornadoes, squall lines, thunderstorms, and other severe local convective phenomena (Norman, Oklahoma).
- WPL** *Wave Propagation Laboratory.* Research areas include: theoretical research on radio waves, optical waves, and acoustic gravity waves; experimental research and development on new forms of remote sensing.
- ARL** *Air Resources Laboratories.* Research areas include: diffusion, transport, and dissipation of atmospheric contaminants; development of methods for prediction and control of atmospheric pollution; geophysical monitoring for climatic change (Silver Spring, Maryland).
- AL** *Aeronomy Laboratory.* Research areas include: theoretical, laboratory, rocket, and satellite studies of the physical and chemical processes controlling the ionosphere and exosphere of the Earth and other planets, and of the dynamics of their interactions with high-altitude meteorology.
- SEL** *Space Environment Laboratory.* Research areas include: solar-terrestrial physics, service and technique development in the areas of environmental monitoring and forecasting.

NATIONAL OCEANIC AND ATMOSPHERIC ADMINISTRATION

BOULDER, COLORADO 80302